SINGLE HELIOSTAT WIND-TUNNEL LOAD VERIFICATION TEST

by

J. E. Cermak[1]

J. A. Peterka[2]

for

McDonnell Douglas Astronautics Company
5301 Bolsa Avenue
Huntington Beach, California 92647

Engineering Sciences

MAR 1 8 1980

Branch Library

Fluid Mechanics and Wind Engineering Program
Fluid Dynamics and Diffusion Laboratory
Department of Civil Engineering
Colorado State University
Fort Collins, Colorado 80523

October 1979

[1]Professor-in-Charge, Fluid Mechanics and Wind Engineering Program
[2]Associate Professor

CER79-80JEC-JAP23

U18401 0077473

TABLE OF CONTENTS

LIST OF TABLES

LIST OF FIGURES

LIST OF SYMBOLS

A_{ref} = constant area, 0.852 ft^2 model

$C_{F_x}, C_{F_y}, C_{F_z}$ = nondimensional force coefficients in x, y and z directions, respectively

$C_{m_z}, C_{m_x}, C_{m_y}$ = nondimensional moment coefficients about the base z, x, y axes, respectively

C_{mh_x}, C_{mh_y} = nondimensional moment coefficients about hinge x and y axes, respectively

C_{mu_x}, C_{mu_y} = nondimensional moment coefficient about upper point x and y axes, respectively,

D = characteristic length (structure height, width, etc.)

F = force along chosen axis

F_x, F_y, F_z = measured force along x, y and z axes, respectively

L_{ref} = reference length, 0.968 ft model

M = moment about chosen axis

M_z, M_x, M_y = measured moment about z, x, and y axes, respectively

M_{h_x}, M_{h_y} = measured hinge moment about x and y axes, respectively

M_{u_x}, M_{u_y} = measured upper-point moment about x and y axes, respectively

U = local mean velocity

U_R = reference mean velocity 1.20 feet model above floor

U_∞ = reference free stream mean velocity at 4.16 feet model above floor

x,y = mutually perpendicular horizontal coordinates

z = vertical coordinate

LIST OF SYMBOLS (continued)

α = tilt angle of heliostat reflector plates

β = incident wind direction

ν = kinematic viscosity of air

ρ = density of air

$\frac{UD}{\nu}$ = Reynolds number

$\frac{\rho U_R^2}{2}$ = reference dynamic pressure

ACKNOWLEDGMENTS

Support for this project was supplied by McDonnell Douglas Astronautics Company. A portion of the data acquisition was supervised by Dr. M. Poreh, visiting professor from the Technion, Israel. Much of the data was acquired by Mr. M. Downing. Photographs were obtained under the direction of Mr. J. Garrison.

1. INTRODUCTION

The magnitude of wind loads on heliostats is an important economic consideration in development of fields of heliostats for sunlight concentration. Drive mechanisms must be sized to control motion of the units in the presence of wind. Oversizing drive mechanisms could result in higher unit costs than necessary. Building code specification or aeronautical data cannot adequately predict forces and moments acting on the complicated geometry of the heliostats. In this study, wind loads on a single heliostat model were obtained in a simulated atmospheric boundary layer flow and in a uniform approach flow in order to determine the influence of the shear and turbulence in the approaching wind on loads and to resolve inconsistencies between previous data obtained in a boundary layer flow (1) and data obtained in a uniform flow.

The primary consideration in modeling wind forces on structures in a wind tunnel is that the wind characteristics in the tunnel simulate natural boundary-layer winds at the actual site. In general, this requires that the vertical distribution of mean velocity and turbulence in the wind tunnel boundary layer match those at the site and that the Reynolds numbers of the model and the prototype be equal. In addition, the small-scale structure must be geometrically similar to its prototype. A detailed discussion of these requirements and their implementation in the wind tunnel environment can be found in references 2, 3 and 4.

The construction of a 1:22 scale model of the prototype structure and its immediate surroundings (in this case, a flat, open area), submerged in a turbulent boundary layer satisfied all the above criteria except that of equal Reynolds numbers and similarity of turbulence characteristics. In the Reynolds number $\frac{UD}{\nu}$, ν is the same for both the tunnel and the full-scale structure. Because of this, the wind tunnel air speed, U, would have to be 22 times the full-scale value if the model and prototype Reynolds numbers are to be equal. Testing at such high wind speeds is not possible. However, for Reynolds numbers larger than 2×10^4, there is no significant change in the values of aerodynamic coefficients as the Reynolds number increases. Since typical Reynolds number values are 10^7 -10^8 for full-scale flow and 10^5-10^6 for wind tunnel flow, acceptable flow similarity is achieved without equality of the Reynolds numbers.

At a model scale of 1:24, the larger scales of turbulence in the atmospheric boundary layer are not simulated in the wind tunnel flow. However, because the heliostat geometry is basically that of a flat plate and because the integral scale of the turbulence in the wind tunnel was 2 to 3 times the largest dimension of the model collecter, the influence of the scale of turbulence was not expected to be significant (5). Evidence exists which demonstrates some influence of turbulence intensity on drag of flat plates (5, 6, 7). Because the difference in turbulence intensity between the current simulation and a simulation with complete similarity of turbulence structure is not large, the effects due to turbulence intensity should be of about the same size as the force balance resolution.

2. EXPERIMENTAL CONFIGURATION

2.1 Model

The 1:22 scale heliostat model used for this study is the same one used in the previous study (1). It is shown in Figures 1 and 2. For the tests in the simulated atmospheric flow, the model was placed on a turntable at the downstream end of the Meteorological Wind Tunnel, Figures 3 and 4. A velocity profile characteristic of an open-country environment was generated using spires and a flow trip at the test-section entrance, to thicken the boundary layer to 50 inches, and roughness on the section floor. The roughness was tailored to provide a 0.14 power law mean velocity profile.

For the tests in a uniform approach flow, the model was installed just downwind of the entrance contraction of the Industrial Wind Tunnel, Figure 5. In order to provide a ground plane with the smallest possible boundary layer, the model was installed at floor level 22 in. downstream from the beginning of the test section. The model installed in the wind tunnel is shown in Figure 6.

2.2 Instrumentation-Velocity

Velocity profiles were made with a single hot-film anemometer mounted with its axis horizontal. The instrument used was a Thermo Systems constant temperature anemometer (Model 1050) with a 0.001 in. dia platinum film sensing element 0.020 in. long. Output from the anemometer was directed to an on-line digital data acquisition system consisting of a Hewlett-Packard 21MX mini-computer with disk, Preston Scientific analog-to-digital converter, and several peripheral units including digital tape drive, card reader, printer and plotter. Hot-film data was acquired and analysed under software control.

Calibration of the hot-film anemometer was performed by comparing voltage output to velocity obtained from a nearby pitot tube. The calibration data were fit to a variable-exponent King's Law relation of the form

$$E^2 = A + BU^n$$

where E is the hot-film output voltage, U the velocity and A, B and n are coefficients selected to fit the data. The above relationship was used to determine the mean velocity at measurement points using the measured mean voltage. The fluctuating velocity in the form U_{rms} (root-mean-square velocity) was obtained from

$$U_{rms} = \frac{2\ E\ E_{rms}}{B\ n\ U^{n-1}}$$

where E_{rms} is the root-mean-square voltage output from the anemometer. Turbulence intensity was calculated by dividing U_{rms} by the local mean velocity (U_{rms}/U).

2.3 Instrumentation - Force and Moments

The model was mounted directly on an Inca six-component strain-gage balance. The balance was mounted below the wind-tunnel floor with its axis horizontal. This orientation enabled the lift on the heliostat to be measured (it was not measured in the original study) in addition to the horizontal force components. Because the force component along the axis of the balance is not as reproducable as desirable, one horizontal force (Fy) was obtained by rotating the model on the balance for measurement of that one component before obtaining the remaining five components. Each strain-gauge bridge of the balance was monitored by a Honeywell Accudata 118 Gauge Control/Amplifier unit which supplied excitation of the bridge and amplified the bridge output. The voltage output from each channel was directed to the on-line digital data acquisition system for processing as described above.

Calibration of the balance was performed in a test rig in which known forces and moments could be applied to the balance. A calibration matrix was then developed for reducing the mean output of the strain gauges. The load and strain relationship was linear for the range of loads applied in these tests. In addition, test loads were applied in place in the wind tunnel on a frequent basis to insure the reliability of the measured loads.

The force balance and electronic system are supported by their manufacturer's specifications to be accurate to within 0.1 percent of the full scale. In force coefficient and moment coefficient form (defined below), this would indicate resolution of 0.015 in force coefficient and 0.015 in moment coefficient. In actual practice, the immediate reproducibility (one data run immediately following another without change of any experimental variables) tended to have better resolution than that quoted. When experimental variables were allowed to vary between tests to check reproducibility (turning velocity off, then back on; changing heliostat elevation angles and azimuth angles, then returning to original position), the quoted resolution limits were approximately correct for force coefficients and slightly low for moment coefficients.

Force and moment coefficients are reported herein to three decimal places since the third place probably has some meaning for a large percentage of the data.

2.4 Force and Moment Coefficients

The forces and moments measured on the heliostat model were expressed, respectively, in terms of the nondimensional coefficients C_F, C_m, C_{mh} and C_{mu}. They are defined as follows:

force coefficient along the x-axis

$$C_{F_x} = \frac{F_x}{\left(\frac{\rho U_R^2}{2}\right)(A_{ref})} ,$$

force coefficient along the y-axis

$$C_{F_y} = \frac{F_y}{\left(\frac{\rho U_R^2}{2}\right)(A_{ref})} ,$$

force coefficient along the z-axis

$$C_{F_z} = \frac{F_z}{\left(\frac{\rho U_R^2}{2}\right)(A_{ref})} ,$$

moment coefficient about the X-axis at the base of the model

$$C_{m_x} = \frac{M_x}{\left(\frac{\rho U_R^2}{2}\right)(A_{ref})\ (L_{ref})},$$

moment coefficient about the y-axis at the base of the model

$$C_{m_y} = \frac{M_y}{\left(\frac{\rho U_R^2}{2}\right)(A_{ref})\ (L_{ref})},$$

moment coefficient about the z-axis

$$C_{m_z} = \frac{M_z}{\left(\frac{\rho U_R^2}{2}\right)(A_{ref})\ (L_{ref})},$$

moment coefficient about the x-axis at the hinge

$$C_{mh_x} = \frac{M_{h_x}}{\left(\frac{\rho U_R^2}{2}\right)(A_{ref})\ (L_{ref})},$$

moment coefficient about the y-axis at the hinge

$$C_{mh_y} = \frac{M_{h_y}}{\left(\frac{\rho U_R^2}{2}\right)(A_{ref})\ (L_{ref})},$$

moment coefficient about the x-axis at the upper point

$$C_{mu_x} = \frac{M_{u_x}}{\left(\frac{\rho U_R^2}{2}\right)(A_{ref})\ (L_{ref})},$$

moment coefficient about the y-axis at the upper point

$$C_{mu_y} = \frac{M_{u_y}}{\left(\frac{\rho U_R^2}{2}\right)(A_{ref})\,(L_{ref})} ,$$

In these equations, the x, y and z axes through the base, hinge and upper point are defined in Figure 7.

F_x, F_y, F_z = measured force along the x, y and z axes,

M_x, M_y, M_z = measured moment about the x, y and z axes at the base,

M_{h_x}, M_{h_y} = measured hinge moment about the x and y axes at the hinge,

M_{u_x}, M_{u_y} = measured upper-point moment about the x and y axes at the upper point,

$A_{(ref)}$ = reference area (0.852 ft^2 model),

$L_{(ref)}$ = reference length (0.968 ft model),

ρ = density of air,

U_R = reference velocity.

The reference velocity, U_R, for the measurements in the boundary layer was the velocity at 1.2 ft above the floor in the approach boundary layer profile (equal to 0.81 U_∞ where U_∞ was the velocity at the pitot-static tube measurement location 50 in. above the wind-tunnel floor). The reference velocity, U_R, for the uniform flow case was the average velocity in the approach flow over the model height (equal to 1.06 U_∞ where U_∞ was the velocity at the pitot-static tube measurement location 48 in. above the wind-tunnel floor. The velocity at U_∞ was was measured using a Setra pressure transducer to monitor the difference between static and dynamic pressure on the pitot-static probe mounted at either 48 or 50 inches above the floor as described above. The Setra transducer was calibrated against a standard maintained by the Engineering Research Center at Colorado State University which is traceable to standards maintained by the National Bureau of Standards.

The upper-point moments were calculated for a point on the upper surface of the heliostat reflector plates 6.72 in. from the tunnel floor for the model. The hinge moments were calculated at the heliostat hinge, 6.07 in. from the tunnel floor for the model. The remaining moments were calculated at the base of the heliostat at floor level.

3. RESULTS

3.1 Velocity

The approach mean velocity profile in the boundary layer flow in the meteorological wind tunnel was obtained at the model location without the model in place. This profile, called MTBYL1, is shown in Figure 8 and is tabulated in Table 1. This mean velocity profile is a 0.14 power law profile. In order to see the influence of the model on the flow immediately in front of the model at $\alpha = 90^{\circ}$ and $\beta = 0^{\circ}$, velocity profiles were obtained on the wind tunnel centerline 1 in. upstream from the plane of the collector mirror surface with the collector in place (profile COLLIN) and at the same location with the collector removed (profile COLOUT). These two profiles are plotted in Figure 9 and are tabulated in Tables 2 and 3. The presence of a stagnation region in front of the collector is clearly evident in Figure 9.

Flow visualization photographs were obtained in the region of the velocity profiles upstream of the heliostat in the boundary layer flow. Figure 10a shows the flow at two different times. Visual inspection showed an unsteady flow which was predominantly through the center slot in the heliostat for a part of the time and predominantly downward as though the slot were blocked for part of the time. Figure 10b shows flow near the floor at two different times. Part of the time, the flow in front of the heliostat was drawn under the heliostat while at other times, the flow tended to roll up into a horseshoe vortex with little flow underneath the heliostat. No marked periodicity was noted in the unsteadiness in the flow.

Velocity profiles obtained in the Industrial Aeordynamics wind tunnel on the centerline 1 in. upstream of the heliostat for $\alpha = 90^o$, $\beta = 0^o$ are shown in Figure 11 and tabulated in Tables 4 and 5. The two profiles represent conditions with the heliostat in place (UFCOLI) and removed (UFCOLO). The uniform approach flow and stagnation region in front of the collector are clearly visiable.

3.2 Heliostat Loads

Force and moment coefficients for the heliostat in the boundary layer flow and uniform flow are listed in Tables 7 and 8 respectively. A plot of CFX for the boundary layer flow case is shown in Figure 12. The shape of the curves for the uniform flow case is similar.

Table 8 shows the ratio of uniform flow to boundary layer flow coefficients for all cases where the boundary layer flow coefficient had a value of 0.05 or larger. If the only difference in coefficient for the two flow conditions were due to assignment of the reference pressure $\rho U_R^2/2$ to an elevation of 1.2 ft above the floor instead of the hinge height at 0.51 ft above the floor, the ratio of coefficients in Table 8 would be the square of the ratio of velocities at the two heights:

$$R = \left(\frac{U_{1.20}}{U_{0.51}}\right)^2 = \left(\frac{Z_{1.2}}{Z_{0.51}}\right)^{(.14)(2)} = \left(\frac{1.2}{0.51}\right)^{0.28} = 1.27$$

The range of ratios found in Table 8 indicate that the presence of shear and turbulence in the approach flow does, as expected, cause differences in loading on the heliostat.

In Table 8, for wind directions near $\beta = 90^o$, some coefficient ratios drop below one indicating higher relative loads for the shear-flow case. The reason for this cannot be determined from data obtained in this study but may be related to the different nature of the separated shear layer over the heliostat due to the presence of turbulence in the approach flow (5,6,7).

3.3 Comparison with Previous Results

The drag coefficient of a square flat plate in uniform flow is about 1.14(8). The drag coefficient on the heliostat at $\alpha = 90^{o}$ and $\beta = 0^{o}$ was measured as 1.17 for the uniform flow indicating that the presence of the slot and ground plane have second-order influence on the drag force--at least in uniform flow.

Comparison of the data of this report with that of reference 1 indicates that the force data and moment data about the base are approximately a constant factor of 0.73 times the data of reference 1. Several possible error sources in the original study were investigated. These sources were 1) the original balance calibration/ data reduction procedure, 2) the possibility that the velocity profile in the original study has a lower exponent than was actually measured and 3) the velocity measurement technique.

To check possibility 1), voltage readings recorded during the original study were processed through the current data reduction procedure including use of the current calibration. Loads reported in the original report were recovered within a few percent. This indicates that original forces and moments were processed correctly and that the balance and supporting electronics are stable to within a few percent over a one year period. An approximate analysis of the influence of a 0.08 power law profile (a steeper profile than has been produced in the meteorological wind tunnel indicates a maximum error of about 12 percent--significantly less than the difference which appears between current data and that of reference 1.

The third possibility, an error in velocity measurement, could occur in one of three ways: (a) human error in setting the offset on the Baratron pressure transducer, (b) the Baratron pressure transducer out of calibration, or (3) a leak in the tygon tubing connecting the pitot-static tube to the pressure transducer. While neither (a) nor (b) can be conclusively ruled out, they are not likely the source of error for several reasons. The ratios of coefficients from the current study to those of reference 1 were not constant within the measurement precision demonstrated in this current study (they showed a standard deviation of 5-7 times the resolution quoted above)--indicating a dispersion of error about a mean. Since several individuals, each trained in the use of the pressure transducer, set the wind-tunnel speed, it is not likely that a constant offset with some dispersion would have occurred. While the periodic re-calibration of the Baratron pressure transducer is performed in such a way that a drift in calibration in service would not be detected, neither of the two Baratron transducers in our laboratory has exhibited this type of error before or since the experiment of reference 1. Thus, the most likely error source in the original experiment was (c) above--a leak in the tubing between the pitot-static tube and pressure transducer, possibly at a coupling. A leak could exhibit an offset in the correct direction with some dispersion. Complete confirmation of the error source cannot be made; hence the true error source cannot be determined with absolute certainty.

Since all data of reference 1 was obtained during a single wind-tunnel experiment in which the tubing to the pitot-static tube was not changed, force data and moment data about the base of reference 1 can be corrected by a factor of 0.73 with reasonable confidence.

Moment coefficients calculated about the hinge or upper point were generally small values since the center of pressure was close to these axes. Since the values are small, the percentage error in those values are much larger than for forces or moments about the base. Ratios of moment coefficients about the hinge or upper point for this study to those of reference 1 give a ratio of 0.99 indicating a systematic deviation of the forces and moments about the base resulting from those forces from the mean ratio of 0.73. Systematic variations within the measurement tolerance of 0.015 in force and base moment coefficient can lead to a 0.99 ratio in hinge and upper point moments. Thus, hinge and upper point moments in reference 1 should not be corrected.

Caution should be exercised in use of the hinge and upper point moment data for design purposes. It is likely that the instantaneous fluctuating moment is much larger--fluctuating both positively and negatively--than the mean value which, on a time average, is quite small.

4. CONCLUSIONS

On the basis of the discussion of Chapter 3, the following conclusions can be drawn:

1. The wind load on a single heliostat perpendicular to a uniform flow is close to that predicted by a solid square flat plate in uniform flow.

2. The wind load on a single heliostat in a simulated atmospheric flow is smaller for most angle orientations than that of a heliostat in a uniform flow based on wind magnitude measured slightly above the top of the heliostat.

3. For some heliostat wind angles, wind loads on the heliostat in the shear flow were relatively larger than those on the heliostat in the uniform flow due, possibly, to the different character of the separated shear layer near the heliostat due to turbulence in the approach boundary layer.

4. Heliostat loads in the boundary layer flow in this study differed from those in a previous study due, as closely as could be determined, to a leak in a pressure transmission line or to an undiscovered drift in an instrument calibration.

REFERENCES

1. Cermak, J. E., Peterka, J. A. and Kareem A., "Heliostat Field-Array Wind-Tunnel Test," Technical Report for McDonnell Douglas Astronautics, CER78-79JEC-JAP-AK2, Fluid Mechanics and Wind Engineering Program, Colorado State University, July 1978.

2. Cermak, J. E., "Aerodynamics of Buildings," Annual Review of Fluid Mechanics, Vol. 8, 1976.

3. Cermak, J. E., "Laboratory Simulation of the Atmospheric Boundary Layer," AIAA Jl., Vol. 9, September 1971.

4. Cermak, J. E., "Applications of Fluid Mechanics to Wind Engineering," A Freeman Scholar Lecture, ASME Jl. of Fluids Engineering, Vol. 97, No. 1, March 1975.

5. Bearman, P. W., Turbulence Effects on Bluff Body Mean Flow, Third U.S. National Conference on Wind Engineering Research, pp. 265-272, 1978.

6. Bearman, P. W., An Investigation of the Forces on Flat Plates Normal to a Turbulent Flow, Jl. Fluid Mechanics, Vol. 46, pp. 177-198, 1971.

7. Nakamura, Y. and Tomonari, Y., The Effect of Turbulence on the Drag of Rectangular Prisms, Transactions Japan Society of Aeronautical and Space Science, Vol. 19, pp. 81-86, 1976.

8. Fail, R., J. A. Lawford, and R. C. W. Eyre, "Low Speed Experiments on the Wake Characteristics of Flat Plates Normal to an Air Stream," Aeronautical Research Council Reports and Memoranda No. 3120, 1959.

Table 1. Velocity Profile in the Meteorological Wind Tunnel at the Model Location

RESULTS FOR PROFILE - MTBYL1

REFERENCE VELOCITY = 92.34 FT/S

HREF = 50.00 IN
HMAX = 50.00 IN

EXPONENT = .1339 U(HMAX) = 90.48

DATA POINT	HEIGHT IN	UMEAN FT/S	U-RMS FT/S	TURB INT PERCENT
1	.25	44.89	8.734	19.46
2	.48	48.54	9.042	18.63
3	.99	54.34	9.850	18.13
4	2.03	58.54	9.325	15.93
5	3.05	62.80	8.946	14.24
6	4.04	64.39	8.039	12.49
7	5.05	67.47	8.276	12.27
8	6.98	68.44	8.127	11.87
9	9.95	71.98	8.227	11.43
10	11.96	73.09	7.895	10.80
11	14.95	75.39	7.681	10.19
12	19.95	78.74	7.682	9.76
13	24.94	81.89	7.882	9.63
14	29.94	84.12	7.592	9.03
15	34.95	87.63	6.599	7.53
16	39.91	90.37	5.942	6.58
17	50.00	92.34	4.288	4.64

Table 2. Velocity Profile in the Meteorological Wind Tunnel with the Heliostat in Place

NORMALIZED PROFILE - COLLIN

REFERENCE VELOCITY = 72.80 FT/S

HREF = 49.96 IN
HMAX = 49.96 IN

HEIGHT NORMALIZED BY HMAX
VELOCITY NORMALIZED BY U(HMAX)

DATA POINT	HEIGHT RATIO	UMEAN RATIO	U-RMS RATIO	TURB INT PERCENT
1	.01	.13	.058	45.19
2	.02	.19	.075	40.30
3	.03	.22	.074	32.84
4	.04	.25	.073	29.93
5	.05	.26	.072	27.91
6	.06	.26	.070	26.57
7	.07	.26	.068	25.85
8	.08	.27	.069	25.18
9	.10	.27	.066	24.57
10	.12	.27	.064	23.34
11	.16	.30	.063	21.03
12	.20	.35	.068	19.43
13	.24	.46	.068	14.68
14	.32	.72	.080	11.07
15	.40	.81	.079	9.74
16	.50	.87	.075	8.67
17	.60	.90	.069	7.69
18	.70	.93	.068	7.35
19	.80	.95	.057	5.95
20	.90	.97	.052	5.32
21	1.00	.97	.048	4.94

Table 3. Velocity Profile in the Meteorological Wind Tunnel with the Heliostat Removed

NORMALIZED PROFILE - COLOUT

REFERENCE VELOCITY = 72.89 FT/S

HREF = 50.09 IN
HMAX = 50.09 IN

EXPONENT = .1364 U(HMAX) = 73.20

HEIGHT NORMALIZED BY HMAX
VELOCITY NORMALIZED BY U(HMAX)

DATA POINT	HEIGHT RATIO	UMEAN RATIO	U-RMS RATIO	TURB INT PERCENT
1	.01	.54	.090	16.63
2	.02	.59	.095	16.24
3	.03	.62	.102	16.42
4	.04	.64	.099	15.53
5	.05	.67	.089	13.42
6	.06	.69	.099	14.29
7	.07	.70	.093	13.28
8	.08	.70	.093	13.35
9	.10	.74	.089	12.06
10	.12	.73	.091	12.52
11	.16	.76	.087	11.40
12	.20	.78	.088	11.25
13	.24	.82	.087	10.72
14	.32	.84	.080	9.54
15	.40	.87	.082	9.38
16	.50	.90	.080	8.80
17	.60	.94	.080	8.55
18	.70	.96	.068	7.09
19	.80	1.00	.061	6.14
20	.90	1.01	.051	5.02
21	1.00	1.00	.057	5.72

Table 4. Velocity Profile in the Industrial Aerodynamics Wind Tunnel with the Heliostat in Place

RESULTS FOR PROFILE - UFCOLI

PITOT TUBE REFERENCE VELOCITY = 65.96 FT/S

HREF = 48.00 IN
HMAX = 48.09 IN

DATA POINT	HEIGHT IN	UMEAN FT/S	U-RMS FT/S	TURB INT PERCENT
1	.25	14.66	7.799	53.20
2	.60	11.71	6.337	54.09
3	1.05	17.77	6.052	34.06
4	1.58	27.29	4.055	14.86
5	1.89	29.36	3.117	10.61
6	2.58	30.24	1.654	5.47
7	3.09	29.44	1.204	4.09
8	4.08	27.49	.823	2.99
9	5.08	25.43	.683	2.69
10	7.11	25.91	.414	1.60
11	9.12	28.21	.363	1.29
12	11.89	36.72	.477	1.30
13	16.12	61.20	.354	.58
14	20.11	67.02	.675	1.01
15	24.08	68.50	.667	.97
16	28.09	68.53	.600	.88
17	33.10	68.58	.661	.96
18	40.09	68.83	.594	.86
19	48.09	69.29	.459	.66

Table 5. Velocity Profile in the Industrial Aerodynamics Wind Tunnel with the Heliostat Removed

RESULTS FOR PROFILE - UFCOLO

PITOT TUBE REFERENCE VELOCITY = 63.98 FT/S

HREF = 48.00 IN
HMAX = 48.08 IN

DATA POINT	HEIGHT IN	UMEAN FT/S	U-RMS FT/S	TURB INT PERCENT
1	.25	48.58	5.019	10.33
2	.58	58.08	4.498	7.75
3	1.07	66.79	1.262	1.89
4	1.59	67.67	.830	1.23
5	1.88	67.57	.823	1.22
6	2.39	67.87	.803	1.18
7	2.90	67.94	.774	1.14
8	4.07	68.22	.743	1.09
9	4.88	67.60	.808	1.20
10	7.09	67.74	.802	1.18
11	9.10	67.63	.788	1.17
12	12.10	67.36	.941	1.40
13	16.10	66.73	.583	.87
14	20.11	66.33	.474	.71
15	24.11	66.22	.320	.48
16	28.10	65.57	.640	.98
17	33.09	65.54	.704	1.07
18	40.12	65.85	.591	.90
19	48.08	66.28	.454	.68

Table 6a. Force and Moment Coefficients for the Heliostat in the Boundary Layer Flow

RUN #	TILT α	WIND β	CFX	CFY	CFZ	CMX	CMY	CMZ	CHHX	CMHY	CMUX	CMUY
208	-10	0.0	-.121	.002	.356	-.010	-.176	.008	-.009	-.113	-.009	-.106
209	-10	22.5	-.122	.056	.351	-.092	-.156	.008	-.063	-.092	-.060	-.085
210	-10	45.0	-.090	.124	.310	-.135	-.116	.010	-.070	-.069	-.063	-.064
211	-10	67.5	-.054	.131	.173	-.120	-.046	.006	-.051	-.018	-.044	-.015
213	-10	90.0	-.005	.092	.040	-.100	.002	-.012	-.052	.005	-.047	.005
214	-10	112.5	.035	.113	-.039	-.081	.011	-.022	-.022	-.007	-.015	-.009
215	-10	135.0	.095	.114	-.173	-.057	.010	-.017	.003	-.040	.009	-.045
216	-10	157.5	.102	.051	-.239	-.009	.015	-.013	.017	-.039	.020	-.044
217	-10	180.0	.107	.002	-.223	.001	.014	-.002	.002	-.042	.002	-.048
207	0	0.0	-.058	.001	.030	-.005	-.056	.006	-.005	-.025	-.005	-.022
206	0	22.5	-.072	.061	.040	-.054	-.046	.008	-.022	-.009	-.018	-.005
205	0	45.0	-.052	.125	.052	-.097	-.032	.011	-.031	-.005	-.024	-.002
204	0	67.5	-.024	.127	.059	-.099	-.013	.007	-.033	-.001	-.026	.001
203	0	90.0	.008	.110	.030	-.092	-.001	-.003	-.034	-.005	-.028	-.006
202	0	112.5	.025	.118	.063	-.100	.019	-.015	-.038	.006	-.032	.004
199	0	135.0	.062	.123	.071	-.108	.036	-.020	-.043	.003	-.037	-.000
201	0	157.5	.065	.068	.112	-.075	.056	.003	-.040	.022	-.036	.018
197	0	180.0	.074	.003	.046	-.008	.057	-.003	-.006	.019	-.006	.014
188	10	0.0	-.099	.003	-.189	-.010	-.030	.003	-.008	.021	-.008	.027
189	10	22.5	-.107	.039	-.187	-.056	-.042	-.020	-.036	.015	-.034	.021
190	10	45.0	-.085	.109	-.166	-.057	-.022	.010	-.000	.023	.006	.028
191	10	67.5	-.039	.115	-.046	-.079	-.013	.009	-.019	.008	-.013	.010
192	10	90.0	.011	.114	.026	-.092	-.002	.005	-.032	-.008	-.026	-.008
193	10	112.5	.038	.127	.161	-.119	.043	-.011	-.052	.023	-.045	.021
194	10	135.0	.079	.122	.249	-.133	.092	-.017	-.069	.050	-.063	.046
195	10	157.5	.100	.051	.262	-.086	.122	-.009	-.060	.070	-.057	.064
196	10	180.0	.093	.007	.261	-.018	.134	-.001	-.014	.085	-.014	.080
187	30	0.0	-.475	.026	-.754	-.001	-.153	.002	.012	.096	.014	.123
185	30	22.5	-.454	.004	-.712	.041	-.179	-.018	.043	.059	.044	.085
184	30	45.0	-.338	.055	-.516	.028	-.150	-.020	.057	.028	.060	.047
183	30	67.5	-.168	.102	-.217	-.044	-.072	-.001	.009	.016	.015	.026
182	30	90.0	.004	.116	.024	-.069	-.003	.035	-.008	-.004	-.002	-.005
349	30	112.5	.186	.140	.331	-.155	.155	.026	-.082	.057	-.074	.047
348	30	135.0	.362	.120	.593	-.180	.299	.029	-.117	.109	-.111	.089
347	30	157.5	.461	.091	.732	-.157	.401	.021	-.109	.159	-.104	.133
346	30	180.0	.510	.004	.807	-.035	.461	-.011	-.033	.194	-.033	.165
169	45	0.0	-.715	.021	-.676	-.005	-.360	.012	.006	.015	.007	.055
170	45	22.5	-.742	.001	-.697	.053	-.373	-.027	.053	.016	.053	.058
171	45	45.0	-.646	.030	-.602	.056	-.335	-.049	.071	.003	.073	.040
172	45	67.5	-.331	.075	-.295	-.010	-.180	-.019	.029	-.006	.033	.012
173	45	90.0	-.000	.102	.023	-.090	.001	.028	-.036	.001	-.031	.001
174	45	112.5	.315	.145	.345	-.169	.227	.042	-.093	.062	-.085	.044
175	45	135.0	.510	.163	.537	-.195	.380	.045	-.110	.113	-.100	.085
176	45	157.5	.630	.099	.633	-.151	.472	.037	-.099	.142	-.093	.107
177	45	180.0	.677	.001	.674	-.037	.498	-.014	-.036	.143	-.036	.105
168	60	0.0	-.943	.024	-.445	-.011	-.531	.022	.001	-.036	.003	.016
167	60	22.5	-.941	.022	-.445	.019	-.528	-.032	.031	-.035	.032	.018
166	60	45.0	-.912	-.005	-.418	.038	-.521	-.067	.036	-.043	.036	.009
165	60	67.5	-.552	.066	-.227	.007	-.310	-.051	.042	-.021	.046	.010
164	60	90.0	-.019	.100	.016	-.074	-.014	.030	-.022	-.004	-.016	-.003

Table 6b. Force and Moment Coefficients for the Heliostat in the Boundary Layer Flow

RUN #	TILT α	WIND β	CFX	CFY	CFZ	CMX	CMY	CMZ	CMHX	CMHY	CMUX	CMUY
163	60	112.5	.428	.147	.261	-.141	.279	.063	-.064	.054	-.056	.030
162	60	135.0	.638	.172	.354	-.167	.423	.072	-.076	.089	-.067	.053
161	60	157.5	.823	.101	.438	-.130	.554	.062	-.077	.122	-.071	.076
160	60	180.0	.854	-.001	.447	-.031	.568	-.008	-.031	.121	-.031	.073
145	75	0.0	-1.024	.023	-.236	-.004	-.591	.022	.008	-.054	.009	.003
146	75	22.5	-1.013	.020	-.225	.009	-.579	-.032	.020	-.048	.021	.009
147	75	45.0	-.945	.007	-.208	.037	-.545	-.070	.041	-.050	.041	.003
148	75	67.5	-.630	.031	-.118	-.006	-.367	-.067	.010	-.037	.012	-.001
155	75	90.0	-.008	.114	.033	-.067	-.015	.038	-.008	-.011	-.001	-.010
156	75	112.5	.488	.161	.153	-.116	.297	.072	-.032	.042	-.023	.014
157	75	135.0	.717	.169	.208	-.133	.453	.081	-.045	.077	-.035	.037
158	75	157.5	.906	.113	.245	-.103	.582	.071	-.043	.107	-.037	.056
159	75	180.0	.969	.016	.255	-.013	.613	-.012	-.005	.105	-.004	.051
60	90	0.0	-1.094	.090	.053	-.067	-.653	.029	-.020	-.079	-.015	-.018
59	90	22.5	-1.065	0.000	.054	-.024	-.625	-.030	-.024	-.066	-.024	-.007
153	90	45.0	-.945	-.010	.047	-.007	-.553	-.061	-.012	-.058	-.013	-.005
154	90	67.5	-.687	.010	.056	-.035	-.411	-.072	-.030	-.051	-.029	-.012
56	90	90.0	-.028	0.000	.031	-.006	-.015	.035	-.006	-.000	-.006	.001
55	90	112.5	.519	.170	.030	-.098	.303	.064	-.009	.031	.000	.002
54	90	135.0	.735	.180	.022	-.110	.432	.081	-.016	.047	-.005	.006
53	90	157.5	.941	.130	.024	-.081	.560	.079	-.013	.067	-.005	.014
52	90	180.0	.991	0.000	-.008	-.027	.602	-.011	-.027	.083	-.027	.027
152	105	0.0	-1.063	.018	.274	-.009	-.646	.027	.001	-.088	.002	-.029
151	105	22.5	-1.033	.024	.264	-.029	-.607	-.033	-.017	-.065	-.016	-.007
150	105	45.0	-.900	.016	.243	-.024	-.546	-.063	-.016	-.074	-.015	-.024
149	105	67.5	-.670	.044	.199	-.057	-.404	-.073	-.034	-.052	-.032	-.015
140	105	90.0	-.048	.097	.043	-.045	-.026	.030	.006	-.001	.011	.002
138	105	112.5	.469	.151	-.066	-.082	.262	.078	-.003	.016	.005	-.010
139	105	135.0	.692	.174	-.121	-.093	.395	.080	-.002	.032	.008	-.007
136	105	157.5	.888	.117	-.166	-.055	.503	.068	.006	.038	.013	-.012
135	105	180.0	.943	.008	-.180	-.016	.537	-.016	-.012	.043	-.012	-.010
306	120	0.0	-.992	.015	.428	-.011	-.623	.019	-.003	-.103	-.002	-.048
307	120	22.5	-.947	.017	.413	-.032	-.595	-.034	-.023	-.098	-.022	-.045
308	120	45.0	-.873	.008	.396	-.035	-.545	-.062	-.031	-.087	-.030	-.038
309	120	67.5	-.600	.051	.298	-.072	-.374	-.065	-.045	-.059	-.042	-.025
301	120	90.0	-.053	.113	.060	-.043	-.030	.025	.016	-.002	.023	.001
302	120	112.5	.419	.142	-.121	-.068	.239	.070	.007	.019	.015	-.005
303	120	135.0	.655	.155	-.207	-.068	.357	.078	.013	.013	.022	-.023
304	120	157.5	.799	.092	-.271	-.051	.453	.059	-.003	.034	.002	-.011
305	120	180.0	.863	.011	-.298	-.015	.487	-.016	-.009	.034	-.009	-.014
313	135	0.0	-.707	.001	.765	-.018	-.507	.014	-.018	-.137	-.018	-.097
312	135	22.5	-.704	.001	.755	-.048	-.499	-.027	-.047	-.131	-.047	-.091
311	135	45.0	-.644	.006	.710	-.079	-.465	-.046	-.076	-.128	-.075	-.091
310	135	67.5	-.328	.066	.399	-.090	-.231	-.016	-.056	-.059	-.052	-.040
300	135	90.0	-.036	.105	.065	-.041	-.015	.021	.014	.004	.020	.006
299	135	112.5	.277	.148	-.226	-.036	.151	.048	.042	.006	.050	-.010
298	135	135.0	.524	.144	-.462	-.029	.274	.056	.046	-.001	.055	-.030
297	135	157.5	.608	.095	-.538	-.007	.291	.047	.043	-.028	.048	-.062
296	135	180.0	.625	.003	-.549	-.009	.304	-.009	-.008	-.024	-.007	-.059
314	150	0.0	-.498	.023	.846	-.023	-.434	.011	-.011	-.173	-.009	-.145

Table 6c. Force and Moment Coefficients for the Heliostat in the Boundary Layer Flow

RUN #	TILT α	WIND β	CFX	CFY	CFZ	CMX	CMY	CMZ	CMHX	CMHY	CMUX	CMUY
315	150	22.5	-.493	.033	.812	-.049	-.404	-.023	-.031	-.146	-.029	-.118
316	150	45.0	-.374	.029	.658	-.086	-.312	-.020	-.071	-.116	-.070	-.095
317	150	67.5	-.176	.091	.328	-.080	-.139	.004	-.032	-.047	-.027	-.037
291	150	90.0	-.020	.103	.073	-.040	-.009	.017	.014	.001	.019	.002
292	150	112.5	.148	.141	-.203	-.020	.069	.026	.054	-.009	.062	-.017
293	150	135.0	.302	.136	-.473	.009	.129	.035	.080	-.029	.088	-.046
294	150	157.5	.394	.081	-.614	.026	.134	.030	.068	-.072	.073	-.095
295	150	180.0	.409	.010	-.653	.003	.118	-.003	.008	-.096	.009	-.119
321	170	0.0	-.100	-.002	.338	-.007	-.108	.004	-.008	-.056	-.008	-.050
320	170	22.5	-.096	.030	.332	-.043	-.104	.012	-.027	-.053	-.026	-.048
319	170	45.0	-.077	.096	.274	-.072	-.079	.021	-.022	-.039	-.017	-.035
318	170	67.5	-.043	.123	.152	-.056	-.029	.021	.009	-.007	.015	-.004
290	170	90.0	.001	.108	.070	-.027	-.008	.012	.030	-.009	.036	-.009
289	170	112.5	.035	.128	-.059	-.024	.016	.000	.043	-.002	.050	-.004
288	170	135.0	.083	.129	-.176	-.020	.015	-.004	.048	-.028	.055	-.033
287	170	157.5	.100	.057	-.206	.002	.003	.001	.032	-.049	.035	-.055
286	170	180.0	.108	-.007	-.190	-.010	-.012	.001	-.013	-.068	-.014	-.074
322	180	0.0	-.060	-.009	.102	-.013	-.017	.002	-.018	.014	-.019	.018
323	180	22.5	-.052	.062	.082	-.031	-.025	.013	.001	.003	.005	.006
324	180	45.0	-.045	.120	.065	-.056	-.023	.023	.007	.001	.014	.003
325	180	67.5	-.020	.133	.055	-.038	-.010	.016	.031	.000	.039	.001
281	180	90.0	-.004	.102	.057	-.030	.000	.003	.023	.002	.029	.003
282	180	112.5	.024	.123	.039	-.044	.011	-.011	.020	-.001	.027	-.002
283	180	135.0	.036	.120	.031	-.054	.023	-.013	.009	.004	.015	.002
284	180	157.5	.057	.060	.038	-.027	.015	-.008	.004	-.015	.008	-.018
285	180	180.0	.058	.009	.036	-.001	.008	-.001	.004	-.022	.004	-.026
330	190	0.0	-.108	-.014	-.205	-.005	.028	.001	-.012	.085	-.013	.091
331	190	22.5	-.101	.041	-.216	.000	.016	.007	.021	.069	.024	.075
332	190	45.0	-.082	.102	-.194	-.026	.000	.012	.027	.043	.033	.048
333	190	67.5	-.040	.123	-.085	-.029	-.006	.009	.036	.015	.043	.017
280	190	90.0	-.013	.105	.068	-.033	-.001	.005	.022	.005	.028	.006
279	190	112.5	.038	.136	-.055	-.019	.013	-.001	.052	-.007	.060	-.009
278	190	135.0	.074	.123	-.167	-.024	.015	-.006	.041	-.023	.048	-.027
277	190	157.5	.095	.073	-.201	.003	.001	-.002	.041	-.049	.045	-.054
276	190	180.0	.099	-.001	-.195	-.000	-.010	.001	-.001	-.062	-.001	-.067

Table 7a. Force and Moment Coefficients for the Heliostat in the Uniform Flow

RUN #	TILT α	WIND β	CFX	CFY	CFZ	CMK	CMY	CMZ	CMHX	CMHY	CMUX	CMUY
963	-10	0.0	-.138	-.000	.381	-.028	-.164	.000	-.028	-.092	-.028	-.084
964	-10	22.5	-.130	.079	.357	-.123	-.141	.002	-.081	-.073	-.077	-.065
965	-10	45.0	-.123	.151	.342	-.172	-.102	-.003	-.093	-.038	-.085	-.031
966	-10	67.5	-.065	.155	.180	-.161	-.042	-.003	-.079	-.007	-.070	-.004
829	-10	90.0	.002	.126	.055	-.129	-.003	-.013	-.063	-.004	-.056	-.004
828	-10	112.5	.036	.152	-.024	-.111	.018	-.028	-.031	-.000	-.023	-.002
827	-10	135.0	.105	.160	-.191	-.083	.017	-.024	.001	-.039	.010	-.044
826	-10	157.5	.134	.064	-.284	-.028	.028	-.012	.006	-.042	.009	-.049
825	-10	180.0	.135	.005	-.254	.004	.029	-.001	.006	-.041	.007	-.049
962	0	0.0	-.091	.009	.047	-.006	-.077	.002	-.001	-.029	-.000	-.024
961	0	22.5	-.078	.082	.058	-.090	-.081	.013	-.047	-.040	-.043	-.036
960	0	45.0	-.065	.165	.075	-.144	-.054	.011	-.057	-.020	-.048	-.016
959	0	67.5	-.038	.151	.070	-.138	-.021	.006	-.059	-.001	-.051	.001
830	0	90.0	.004	.118	.034	-.132	.004	-.001	-.070	.002	-.063	.002
831	0	112.5	.038	.149	.080	-.141	.024	-.019	-.063	.004	-.055	.002
832	0	135.0	.062	.166	.059	-.139	.053	-.027	-.052	.021	-.043	.017
833	0	157.5	.068	.077	.033	-.076	.082	-.020	-.036	.046	-.031	.042
834	0	180.0	.098	.001	.016	-.007	.067	-.000	-.006	.015	-.006	.010
954	10	0.0	-.132	.008	-.243	.005	-.046	-.001	.009	.023	.010	.031
955	10	22.5	-.126	.072	-.290	-.033	-.054	.011	.005	.012	.009	.019
956	10	45.0	-.097	.152	-.191	-.093	-.038	.014	-.014	.013	-.005	.018
958	10	67.5	-.045	.136	-.037	-.122	-.020	.018	-.051	.003	-.043	.006
839	10	90.0	.020	.133	.021	-.119	-.002	.012	-.049	-.013	-.041	-.014
838	10	112.5	.061	.161	.190	-.157	.054	-.007	-.073	.022	-.064	.019
837	10	135.0	.114	.155	.342	-.166	.125	-.010	-.084	.065	-.076	.059
836	10	157.5	.120	.079	.354	-.108	.171	-.007	-.066	.108	-.062	.101
835	10	180.0	.146	-.004	.373	-.019	.187	-.003	-.021	.111	-.021	.102
953	30	0.0	-.648	-.019	-.942	-.006	-.249	.009	-.016	.091	-.017	.127
952	30	22.5	-.599	.015	-.861	.075	-.267	-.024	.083	.047	.084	.081
951	30	45.0	-.461	.070	-.643	.039	-.212	-.030	.076	.030	.080	.056
950	30	67.5	-.202	.125	-.271	-.049	-.096	-.001	.016	.010	.023	.021
840	30	90.0	.006	.126	-.002	-.112	-.001	.029	-.046	-.004	-.039	-.005
841	30	112.5	.190	.183	.323	-.171	.167	.017	-.075	.067	-.065	.056
842	30	135.0	.397	.191	.620	-.190	.286	.031	-.090	.077	-.079	.055
843	30	157.5	.542	.111	.842	-.170	.421	.038	-.112	.137	-.105	.106
844	30	180.0	.605	-.012	.930	-.030	.473	.002	-.036	.156	-.037	.122
1031	45	0.0	-.799	.006	-.772	-.025	-.400	.014	-.022	.019	-.022	.064
1032	45	22.5	-.762	.012	-.739	.029	-.387	-.024	.035	.012	.036	.055
1035	45	45.0	-.724	.032	-.690	.043	-.387	-.042	.060	-.007	.062	.034
1036	45	67.5	-.415	.111	-.378	-.014	-.206	-.031	.044	.012	.050	.035
849	45	90.0	-.007	.118	-.018	-.103	-.013	.037	-.041	-.009	-.035	-.009
848	45	112.5	.322	.192	.327	-.172	.231	.035	-.071	.062	-.060	.044
847	45	135.0	.546	.215	.528	-.190	.356	.049	-.077	.070	-.065	.040
846	45	157.5	.741	.129	.712	-.145	.494	.048	-.077	.106	-.070	.064
845	45	180.0	.825	-.010	.789	-.028	.546	-.002	-.034	.114	-.034	.067
945	60	0.0	-.969	.011	-.514	.028	-.509	.011	.034	-.001	.035	.054
944	60	22.5	-.994	-.015	-.527	.049	-.532	-.045	.042	-.011	.041	.045
943	60	45.0	-.952	.019	-.499	.080	-.530	-.069	.090	-.031	.091	.022
942	60	67.5	-.602	.088	-.306	.017	-.321	-.052	.063	-.005	.067	.029
850	60	90.0	-.027	.116	-.019	-.093	-.022	.044	-.032	-.008	-.026	-.006

Table 7b. Force and Moment Coefficients for the Heliostat in the Uniform Flow

RUN #	TILT α	WIND β	CFX	CFY	CFZ	CMX	CMY	CMZ	CMHX	CMHY	CMUX	CMUY
851	60	112.5	.392	.196	.238	-.152	.254	.047	-.049	.049	-.038	.027
852	60	135.0	.715	.216	.424	-.184	.434	.083	-.070	.059	-.058	.019
853	60	157.5	.949	.121	.542	-.127	.568	.071	-.064	.071	-.057	.018
854	60	180.0	1.005	-.011	.565	-.039	.609	.024	-.045	.082	-.045	.026
938	75	0.0	-1.088	.004	-.263	.028	-.611	.020	.030	-.041	.030	.020
939	75	22.5	-1.141	.000	-.256	.042	-.611	-.044	.042	-.013	.042	.051
940	75	45.0	-1.036	.016	-.246	.056	-.582	-.072	.064	-.039	.065	.019
941	75	67.5	-.720	.029	-.170	.005	-.429	-.078	.020	-.052	.022	-.011
859	75	90.0	-.058	.118	-.016	-.073	-.014	.045	-.011	.017	-.005	.020
858	75	112.5	.416	.198	.127	-.129	.246	.068	-.025	.028	-.014	.004
857	75	135.0	.823	.187	.250	-.159	.485	.094	-.061	.053	-.051	.007
856	75	157.5	1.086	.127	.309	-.103	.616	.080	-.036	.047	-.029	-.014
855	75	180.0	1.115	-.021	.307	-.035	.646	.015	-.046	.062	-.047	-.001
865	90	0.0	-1.171	.017	.076	.043	-.635	.009	.052	-.021	.053	.044
866	90	22.5	-1.150	.001	.059	.025	-.640	-.044	.026	-.037	.026	.027
867	90	45.0	-1.059	.008	.051	.033	-.598	-.072	.037	-.043	.038	.016
868	90	67.5	-.825	-.001	.029	-.022	-.479	-.088	-.022	-.046	-.022	.000
860	90	90.0	-.058	.104	-.001	-.059	-.020	.046	-.005	.010	.001	.014
861	90	112.5	.565	.194	.031	-.110	.316	.053	-.009	.020	.002	-.012
862	90	135.0	.872	.190	.051	-.128	.478	.080	-.028	.021	-.018	-.028
863	90	157.5	1.060	.118	.047	-.080	.588	.074	-.018	.032	-.012	-.027
864	90	180.0	1.133	-.015	.040	-.028	.617	.010	-.036	.023	-.037	-.041
937	105	0.0	-1.210	.011	.348	.016	-.667	-.008	.022	-.033	.023	.035
936	105	22.5	-1.140	.052	.325	.018	-.631	-.047	.045	-.033	.048	.031
935	105	45.0	-1.014	.011	.286	-.016	-.569	-.073	-.010	-.038	-.009	.019
934	105	67.5	-.784	.042	.226	-.050	-.468	-.084	-.028	-.057	-.025	-.013
1046	105	90.0	-.051	.119	.001	-.045	-.018	.036	.017	.009	.024	.012
873	105	112.5	.455	.188	-.111	-.099	.238	.055	-.001	-.001	.010	-.026
872	105	135.0	.841	.205	-.195	-.091	.437	.090	.017	-.004	.028	-.051
871	105	157.5	.975	.128	-.221	-.050	.520	.078	.017	.009	.024	-.046
870	105	180.0	1.034	-.004	-.210	-.014	.523	.001	-.016	-.019	-.016	-.077
930	120	0.0	-1.086	-.031	.653	-.024	-.633	-.016	-.040	-.064	-.041	-.003
931	120	22.5	-1.078	.014	.651	-.016	-.628	-.053	-.009	-.062	-.008	-.002
932	120	45.0	-.964	.009	.593	-.044	-.565	-.072	-.039	-.059	-.039	-.005
933	120	67.5	-.628	.055	.389	-.098	-.384	-.065	-.069	-.055	-.066	-.020
875	120	90.0	-.057	.130	.024	-.047	-.023	.028	.021	.007	.028	.011
876	120	112.5	.407	.205	-.185	-.086	.188	.050	.021	-.025	.033	-.048
877	120	135.0	.735	.191	-.351	-.080	.380	.075	.020	-.005	.030	-.046
878	120	157.5	.871	.133	-.424	-.017	.457	.066	.053	.001	.060	-.048
879	120	180.0	.890	-.008	-.417	-.010	.447	-.009	-.014	-.019	-.015	-.069
929	135	0.0	-.889	-.012	.885	-.003	-.555	-.002	-.010	-.089	-.010	-.039
928	135	22.5	-.886	.003	.881	-.038	-.542	-.042	-.036	-.077	-.036	-.028
927	135	45.0	-.795	.016	.805	-.058	-.485	-.060	-.049	-.068	-.048	-.024
926	135	67.5	-.409	.074	.417	-.105	-.257	-.030	-.066	-.043	-.062	-.020
884	135	90.0	-.028	.112	.035	-.053	-.019	.027	.005	-.004	.012	-.003
883	135	112.5	.348	.214	-.300	-.065	.150	.039	.047	-.032	.059	-.052
882	135	135.0	.538	.211	-.471	-.051	.274	.051	.060	-.007	.072	-.038
881	135	157.5	.729	.136	-.631	.002	.326	.053	.073	-.056	.081	-.097
880	135	180.0	.722	-.013	-.618	-.018	.338	-.012	-.025	-.041	-.026	-.081
922	150	0.0	-.617	-.016	1.024	-.007	-.454	-.005	-.015	-.131	-.016	-.096

Table 7c. Force and Moment Coefficients for the Heliostat in the Uniform Flow

RUN #	TILT α	WIND β	CFX	CFY	CFZ	CMX	CMY	CMZ	CMHX	CMHY	CMUX	CMUY
923	150	22.5	-.591	-.006	.969	-.067	-.423	-.039	-.070	-.114	-.070	-.081
924	150	45.0	-.444	.053	.737	-.089	-.331	-.030	-.062	-.099	-.059	-.074
925	150	67.5	-.202	.088	.347	-.104	-.152	-.002	-.058	-.046	-.053	-.035
885	150	90.0	-.004	.121	.035	-.043	-.018	.025	.021	-.015	.028	-.015
886	150	112.5	.218	.200	-.315	-.034	.085	.031	.071	-.029	.082	-.041
887	150	135.0	.408	.197	-.591	-.013	.186	.039	.090	-.028	.101	-.051
888	150	157.5	.540	.125	-.778	.045	.197	.037	.111	-.085	.118	-.116
889	150	180.0	.586	.015	-.841	-.001	.197	-.003	.007	-.111	.008	-.143
921	170	0.0	-.143	-.006	.429	-.007	-.142	.003	-.011	-.067	-.011	-.059
920	170	22.5	-.127	.015	.436	-.093	-.147	.014	-.085	-.080	-.084	-.073
919	170	45.0	-.108	.116	.313	-.092	-.098	.017	-.031	-.041	-.024	-.035
918	170	67.5	-.061	.133	.152	-.071	-.045	.018	-.001	-.013	.007	-.009
894	170	90.0	-.009	.125	.020	-.029	.002	.015	.037	.007	.044	.007
893	170	112.5	.063	.163	-.161	-.026	.023	.005	.059	-.009	.068	-.013
892	170	135.0	.126	.162	-.317	-.032	.031	-.001	.053	-.035	.062	-.042
891	170	157.5	.149	.087	-.352	.002	.013	.002	.048	-.065	.053	-.073
890	170	180.0	.161	.005	-.323	-.003	-.010	.004	-.000	-.094	-.000	-.103
914	180	0.0	-.078	.003	.084	-.004	-.025	.003	-.002	.016	-.002	.020
915	180	22.5	-.074	.074	.076	-.049	-.044	.017	-.010	-.005	-.006	-.001
916	180	45.0	-.072	.170	.042	-.069	-.034	.026	.020	.004	.029	.008
917	180	67.5	-.022	.167	.022	-.039	-.026	.018	.049	-.014	.058	-.013
899	180	90.0	-.006	.132	.009	-.020	.003	.009	.050	.007	.057	.007
900	180	112.5	.035	.151	-.008	-.043	.013	-.009	.036	-.005	.044	-.007
901	180	135.0	.067	.166	.003	-.065	.026	-.017	.022	-.009	.031	-.013
902	180	157.5	.075	.113	.020	-.016	.026	-.008	.043	-.013	.049	-.018
903	180	180.0	.079	-.009	.023	-.010	.011	-.003	-.015	-.030	-.016	-.035
913	190	0.0	-.131	-.016	-.233	-.009	.029	-.000	-.017	.098	-.018	.106
912	190	22.5	-.122	.083	-.260	-.004	.005	.007	.040	.069	.044	.076
911	190	45.0	-.105	.164	-.232	-.039	-.009	.014	.047	.046	.057	.052
910	190	67.5	-.034	.148	-.091	-.033	-.022	.013	.045	-.004	.053	-.002
909	190	90.0	-.000	.134	-.001	-.014	-.001	.001	.056	-.001	.064	-.001
908	190	112.5	.044	.127	.121	-.073	.033	-.012	-.006	.010	.001	.007
907	190	135.0	.100	.124	.289	-.084	.070	-.012	-.019	.017	-.012	.012
906	190	157.5	.113	.039	.388	-.047	.107	-.009	-.027	.048	-.025	.041
905	190	180.0	.137	-.008	.385	-.008	.101	-.001	-.012	.030	-.013	.022

Table 8a. Ratio of Uniform Flow to Boundary Layer Flow Coefficients for Denominator > 0.05

RUN #	TILT α	WIND β	CFX	CFY	CFZ	CMX	CMY	CMZ	CMHX	CMHY	CMUX	CMUY
963	-10	0.0	1.14	0.00	1.07	0.00	.93	0.00	0.00	.81	0.00	.79
964	-10	22.5	1.07	1.41	1.02	1.33	.90	0.00	1.29	.79	1.28	.77
965	-10	45.0	1.36	1.22	1.10	1.28	.88	0.00	1.33	.55	1.35	.49
966	-10	67.5	1.21	1.19	1.04	1.34	0.00	0.00	1.55	0.00	0.00	0.00
829	-10	90.0	0.00	1.37	0.00	1.29	0.00	0.00	1.21	0.00	0.00	0.00
828	-10	112.5	0.00	1.34	0.00	1.37	0.00	0.00	0.00	0.00	0.00	0.00
827	-10	135.0	1.11	1.40	1.10	1.46	0.00	0.00	0.00	0.00	0.00	0.00
826	-10	157.5	1.31	1.25	1.19	0.00	0.00	0.00	0.00	0.00	0.00	0.00
825	-10	180.0	1.25	0.00	1.14	0.00	0.00	0.00	0.00	0.00	0.00	0.00
962	0	0.0	1.57	0.00	0.00	0.00	1.38	0.00	0.00	0.00	0.00	0.00
961	0	22.5	1.08	1.34	0.00	1.68	0.00	0.00	0.00	0.00	0.00	0.00
960	0	45.0	1.26	1.32	1.45	1.48	0.00	0.00	0.00	0.00	0.00	0.00
959	0	67.5	0.00	1.19	1.20	1.39	0.00	0.00	0.00	0.00	0.00	0.00
830	0	90.0	0.00	1.07	0.00	1.43	0.00	0.00	0.00	0.00	0.00	0.00
831	0	112.5	0.00	1.26	1.27	1.41	0.00	0.00	0.00	0.00	0.00	0.00
832	0	135.0	1.00	1.35	.83	1.29	0.00	0.00	0.00	0.00	0.00	0.00
833	0	157.5	1.04	1.13	.30	1.01	1.46	0.00	0.00	0.00	0.00	0.00
834	0	180.0	1.32	0.00	0.00	0.00	1.16	0.00	0.00	0.00	0.00	0.00
954	10	0.0	1.34	0.00	1.29	0.00	0.00	0.00	0.00	0.00	0.00	0.00
955	10	22.5	1.18	0.00	1.55	.59	0.00	0.00	0.00	0.00	0.00	0.00
956	10	45.0	1.14	1.40	1.15	1.63	0.00	0.00	0.00	0.00	0.00	0.00
958	10	67.5	0.00	1.18	0.00	1.54	0.00	0.00	0.00	0.00	0.00	0.00
839	10	90.0	0.00	1.17	0.00	1.29	0.00	0.00	0.00	0.00	0.00	0.00
838	10	112.5	0.00	1.26	1.18	1.32	0.00	0.00	1.39	0.00	0.00	0.00
837	10	135.0	1.44	1.27	1.37	1.24	1.36	0.00	1.21	1.29	1.21	0.00
836	10	157.5	1.20	1.56	1.35	1.25	1.39	0.00	1.11	1.54	1.09	1.57
835	10	180.0	1.56	0.00	1.43	0.00	1.39	0.00	0.00	1.30	0.00	1.28
953	30	0.0	1.36	0.00	1.25	0.00	1.63	0.00	0.00	.94	0.00	1.03
952	30	22.5	1.32	0.00	1.21	0.00	1.49	0.00	0.00	.79	0.00	.95
951	30	45.0	1.36	1.27	1.25	0.00	1.42	0.00	1.34	0.00	1.34	0.00
950	30	67.5	1.20	1.22	1.24	0.00	1.34	0.00	0.00	0.00	0.00	0.00
840	30	90.0	0.00	1.09	0.00	1.63	0.00	0.00	0.00	0.00	0.00	0.00
841	30	112.5	1.02	1.31	.98	1.10	1.07	0.00	.92	1.17	.88	0.00
842	30	135.0	1.10	1.59	1.04	1.05	.96	0.00	.76	.71	.71	.62
843	30	157.5	1.18	1.22	1.15	1.08	1.05	0.00	1.02	.86	1.01	.80
844	30	180.0	1.19	0.00	1.15	0.00	1.03	0.00	0.00	.80	0.00	.74
1031	45	0.0	1.12	0.00	1.14	0.00	1.11	0.00	0.00	0.00	0.00	1.17
1032	45	22.5	1.03	0.00	1.06	.54	1.04	0.00	.66	0.00	.67	.94
1035	45	45.0	1.12	0.00	1.15	.78	1.15	0.00	.84	0.00	.84	0.00
1036	45	67.5	1.25	1.48	1.28	0.00	1.14	0.00	0.00	0.00	0.00	0.00
849	45	90.0	0.00	1.16	0.00	1.15	0.00	0.00	0.00	0.00	0.00	0.00
848	45	112.5	1.02	1.32	.95	1.02	1.02	0.00	.76	1.00	.71	0.00
847	45	135.0	1.07	1.32	.98	.97	.94	0.00	.70	.62	.65	.47
846	45	157.5	1.18	1.31	1.12	.96	1.05	0.00	.78	.74	.75	.60
845	45	180.0	1.22	0.00	1.17	0.00	1.10	0.00	0.00	.79	0.00	.64
945	60	0.0	1.03	0.00	1.16	0.00	.96	0.00	0.00	0.00	0.00	0.00
944	60	22.5	1.06	0.00	1.19	0.00	1.01	0.00	0.00	0.00	0.00	0.00
943	60	45.0	1.04	0.00	1.19	0.00	1.02	1.03	0.00	0.00	0.00	0.00
942	60	67.5	1.09	1.33	1.35	0.00	1.03	1.02	0.00	0.00	0.00	0.00
850	60	90.0	0.00	1.16	0.00	1.25	0.00	0.00	0.00	0.00	0.00	0.00

Table 8b. Ratio of Uniform Flow to Boundary Layer Flow Coefficients for Denominator > 0.05

RUN #	TILT α	WIND β	CFX	CFY	CFZ	CMX	CMY	CMZ	CMHX	CMHY	CMUX	CMUY
851	60	112.5	.92	1.33	.91	1.08	.91	.75	.77	.90	.69	0.00
852	60	135.0	1.12	1.26	1.20	1.10	1.03	1.14	.92	.67	.87	.36
853	60	157.5	1.15	1.20	1.24	.98	1.03	1.14	.83	.58	.80	.23
854	60	180.0	1.18	0.00	1.26	0.00	1.07	0.00	0.00	.68	0.00	.35
938	75	0.0	1.06	0.00	1.11	0.00	1.03	0.00	0.00	.75	0.00	0.00
939	75	22.5	1.13	0.00	1.14	0.00	1.06	0.00	0.00	0.00	0.00	0.00
940	75	45.0	1.10	0.00	1.18	0.00	1.07	1.02	0.00	.78	0.00	0.00
941	75	67.5	1.14	0.00	1.43	0.00	1.17	1.17	0.00	0.00	0.00	0.00
859	75	90.0	0.00	1.04	0.00	1.09	0.00	0.00	0.00	0.00	0.00	0.00
858	75	112.5	.85	1.23	.83	1.11	.83	.94	0.00	0.00	0.00	0.00
857	75	135.0	1.15	1.11	1.20	1.20	1.07	1.17	0.00	.69	0.00	0.00
856	75	157.5	1.20	1.12	1.26	1.00	1.06	1.14	0.00	.44	0.00	-.26
855	75	180.0	1.15	0.00	1.20	0.00	1.05	0.00	0.00	.59	0.00	-.02
865	90	0.0	1.07	.19	1.42	-.64	.97	0.00	0.00	.27	0.00	0.00
866	90	22.5	1.08	0.00	1.10	0.00	1.02	0.00	0.00	.56	0.00	0.00
867	90	45.0	1.12	0.00	0.00	0.00	1.08	1.18	0.00	.75	0.00	0.00
868	90	67.5	1.20	0.00	.52	0.00	1.17	1.23	0.00	.91	0.00	0.00
860	90	90.0	0.00	0.00	0.00	0.00	0.00	0.00	0.00	0.00	0.00	0.00
861	90	112.5	1.09	1.14	0.00	1.12	1.04	.84	0.00	0.00	0.00	0.00
862	90	135.0	1.19	1.06	0.00	1.16	1.11	.99	0.00	0.00	0.00	0.00
863	90	157.5	1.13	.91	0.00	.99	1.05	.94	0.00	.48	0.00	0.00
864	90	180.0	1.14	0.00	0.00	0.00	1.02	0.00	0.00	.28	0.00	0.00
937	105	0.0	1.14	0.00	1.27	0.00	1.03	0.00	0.00	.38	0.00	0.00
936	105	22.5	1.10	0.00	1.23	0.00	1.04	0.00	0.00	.51	0.00	0.00
935	105	45.0	1.13	0.00	1.18	0.00	1.04	1.16	0.00	.51	0.00	0.00
934	105	67.5	1.17	0.00	1.13	.87	1.16	1.16	0.00	1.09	0.00	0.00
1046	105	90.0	0.00	1.22	0.00	0.00	0.00	0.00	0.00	0.00	0.00	0.00
873	105	112.5	.97	1.25	1.68	1.21	.91	.71	0.00	0.00	0.00	0.00
872	105	135.0	1.22	1.18	1.61	.98	1.11	1.12	0.00	0.00	0.00	0.00
871	105	157.5	1.10	1.09	1.33	.91	1.03	1.15	0.00	0.00	0.00	0.00
870	105	180.0	1.10	0.00	1.17	0.00	.97	0.00	0.00	0.00	0.00	0.00
930	120	0.0	1.09	0.00	1.53	0.00	1.02	0.00	0.00	.62	0.00	0.00
931	120	22.5	1.14	0.00	1.57	0.00	1.05	0.00	0.00	.63	0.00	0.00
932	120	45.0	1.10	0.00	1.50	0.00	1.04	1.16	0.00	.68	0.00	0.00
933	120	67.5	1.05	1.09	1.31	1.37	1.03	1.01	0.00	.94	0.00	0.00
875	120	90.0	1.08	1.15	.41	0.00	0.00	0.00	0.00	0.00	0.00	0.00
876	120	112.5	.97	1.44	1.53	1.27	.79	.72	0.00	0.00	0.00	0.00
877	120	135.0	1.12	1.23	1.69	1.18	1.07	.95	0.00	0.00	0.00	0.00
878	120	157.5	1.09	1.44	1.56	.32	1.01	1.12	0.00	0.00	0.00	0.00
879	120	180.0	1.03	0.00	1.40	0.00	.92	0.00	0.00	0.00	0.00	0.00
929	135	0.0	1.26	0.00	1.16	0.00	1.09	0.00	0.00	.65	0.00	.40
928	135	22.5	1.26	0.00	1.17	0.00	1.08	0.00	0.00	.59	0.00	.30
927	135	45.0	1.23	0.0.0	1.13	.73	1.04	0.00	.65	.54	.64	.26
926	135	67.5	1.25	1.11	1.04	1.16	1.12	0.00	1.19	.73	1.20	0.00
884	135	90.0	0.00	1.06	.54	0.00	0.00	0.00	0.00	0.00	0.00	0.00
883	135	112.5	1.26	1.44	1.32	0.00	.99	0.00	0.00	0.00	1.18	0.00
882	135	135.0	1.03	1.46	1.02	0.00	1.00	.92	0.00	0.00	1.32	0.00
881	135	157.5	1.20	1.43	1.17	0.00	1.12	0.00	0.00	0.00	0.00	1.57
880	135	180.0	1.15	0.00	1.13	0.00	1.11	0.00	0.00	0.00	0.00	1.38
922	150	0.0	1.24	0.00	1.21	0.00	1.05	0.00	0.00	.76	0.00	.66

Table 8c. Ratio of Uniform Flow to Boundary Layer Flow Coefficients for Denominator > 0.05

RUN #	TILT α	WIND β	CFX	CFY	CFZ	CMX	CMY	CMZ	CMHX	CMHY	CMUX	CMUY
923	150	22.5	1.20	0.00	1.19	0.00	1.05	0.00	0.00	.78	0.00	.68
924	150	45.0	1.19	0.00	1.12	1.04	1.06	0.00	.87	.85	.84	.78
925	150	67.5	1.15	.97	1.06	1.30	1.09	0.00	0.00	0.00	0.00	0.00
885	150	90.0	0.00	1.18	.49	0.00	0.00	0.00	0.00	0.00	0.00	0.00
886	150	112.5	1.48	1.42	1.55	0.00	1.24	0.00	1.32	0.00	1.33	0.00
887	150	135.0	1.35	1.45	1.25	0.00	1.44	0.00	1.13	0.00	1.16	0.00
888	150	157.5	1.37	1.54	1.27	0.00	1.47	0.00	1.62	1.18	1.62	1.22
889	150	180.0	1.43	0.00	1.29	0.00	1.66	0.00	0.00	1.15	0.00	1.20
921	170	0.0	1.44	0.00	1.27	0.00	1.31	0.00	0.00	1.19	0.00	1.16
920	170	22.5	1.32	0.00	1.31	0.00	1.42	0.00	0.00	1.50	0.00	0.00
919	170	45.0	1.41	1.21	1.14	1.27	1.24	0.00	0.00	0.00	0.00	0.00
918	170	67.5	0.00	1.08	1.00	1.26	0.00	0.00	0.00	0.00	0.00	0.00
894	170	90.0	0.00	1.16	.29	0.00	0.00	0.00	0.00	0.00	0.00	0.00
893	170	112.5	0.00	1.27	2.74	0.00	0.00	0.00	0.00	0.00	1.36	0.00
892	170	135.0	1.52	1.25	1.80	0.00	0.00	0.00	0.00	0.00	1.13	0.00
891	170	157.5	1.50	1.53	1.71	0.00	0.00	0.00	0.00	0.00	0.00	1.34
890	170	180.0	1.48	0.00	1.70	0.00	0.00	0.00	0.00	1.38	0.00	1.38
914	180	0.0	1.31	0.00	.82	0.00	0.00	0.00	0.00	0.00	0.00	0.00
915	180	22.5	1.41	1.19	.93	0.00	0.00	0.00	0.00	0.00	0.00	0.00
916	180	45.0	0.00	1.42	.65	1.24	0.00	0.00	0.00	0.00	0.00	0.00
917	180	67.5	0.00	1.26	.41	0.00	0.00	0.00	0.00	0.00	0.00	0.00
899	180	90.0	0.00	1.30	.16	0.00	0.00	0.00	0.00	0.00	0.00	0.00
900	180	112.5	0.00	1.23	0.00	0.00	0.00	0.00	0.00	0.00	0.00	0.00
901	180	135.0	0.00	1.38	0.00	1.21	0.00	0.00	0.00	0.00	0.00	0.00
902	180	157.5	1.32	1.88	0.00	0.00	0.00	0.00	0.00	0.00	0.00	0.00
903	180	180.0	1.37	0.00	0.00	0.00	0.00	0.00	0.00	0.00	0.00	0.00
913	190	0.0	1.21	0.00	1.13	0.00	0.00	0.00	0.00	1.15	0.00	1.16
912	190	22.5	1.20	0.00	1.20	0.00	0.00	0.00	0.00	1.00	0.00	1.02
911	190	45.0	1.28	1.61	1.20	0.00	0.00	0.00	0.00	0.00	0.00	0.00
910	190	67.5	0.00	1.20	1.08	0.00	0.00	0.00	0.00	0.00	0.00	0.00
909	190	90.0	0.00	1.27	-.01	0.00	0.00	0.00	0.00	0.00	0.00	0.00
908	190	112.5	0.00	.93	-2.20	0.00	0.00	0.00	-.12	0.00	.01	0.00
907	190	135.0	1.36	1.01	-1.72	0.00	0.00	0.00	0.00	0.00	0.00	0.00
906	190	157.5	1.19	.53	-1.92	0.00	0.00	0.00	0.00	0.00	0.00	-.76
905	190	180.0	1.38	0.00	-1.97	0.00	0.00	0.00	0.00	-.48	0.00	-.33

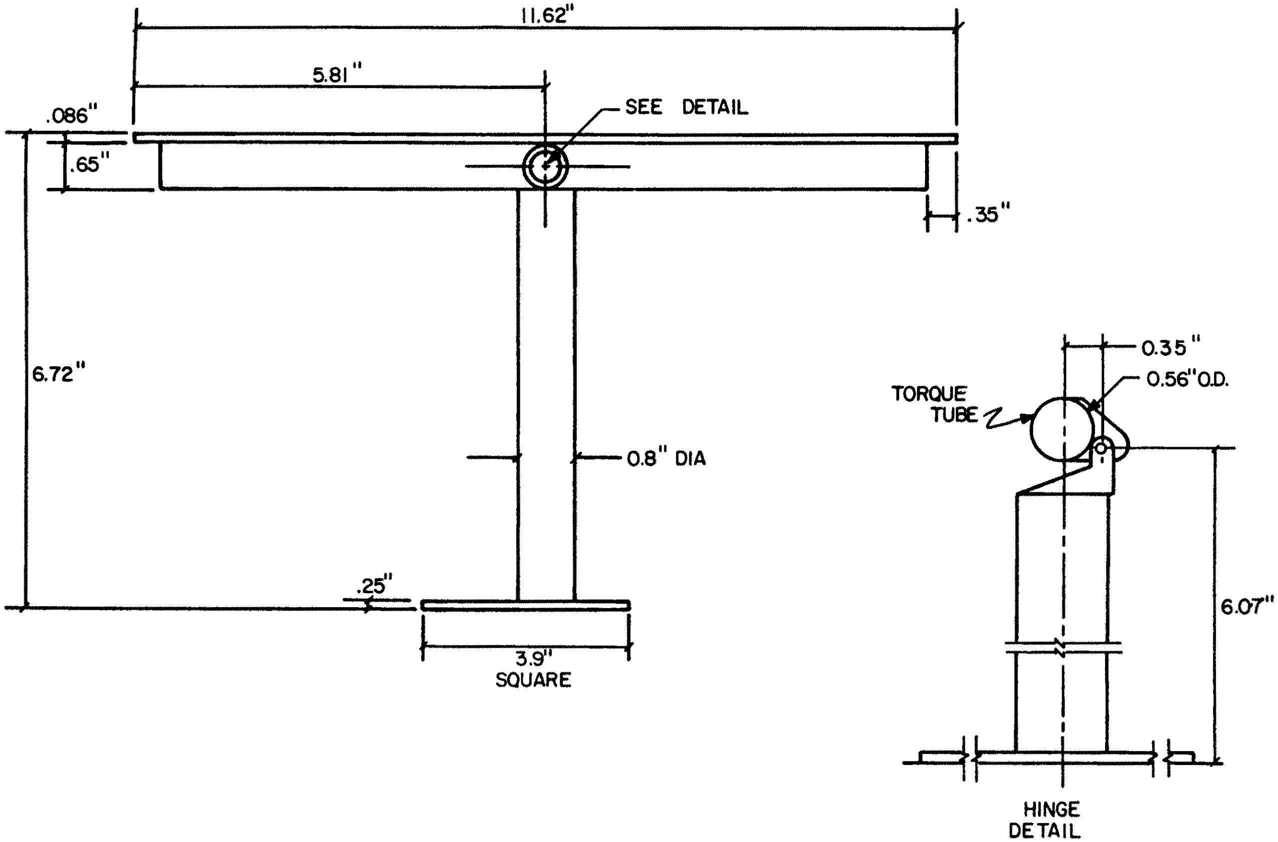

Figure 1a. Heliostat Test Model Dimensions

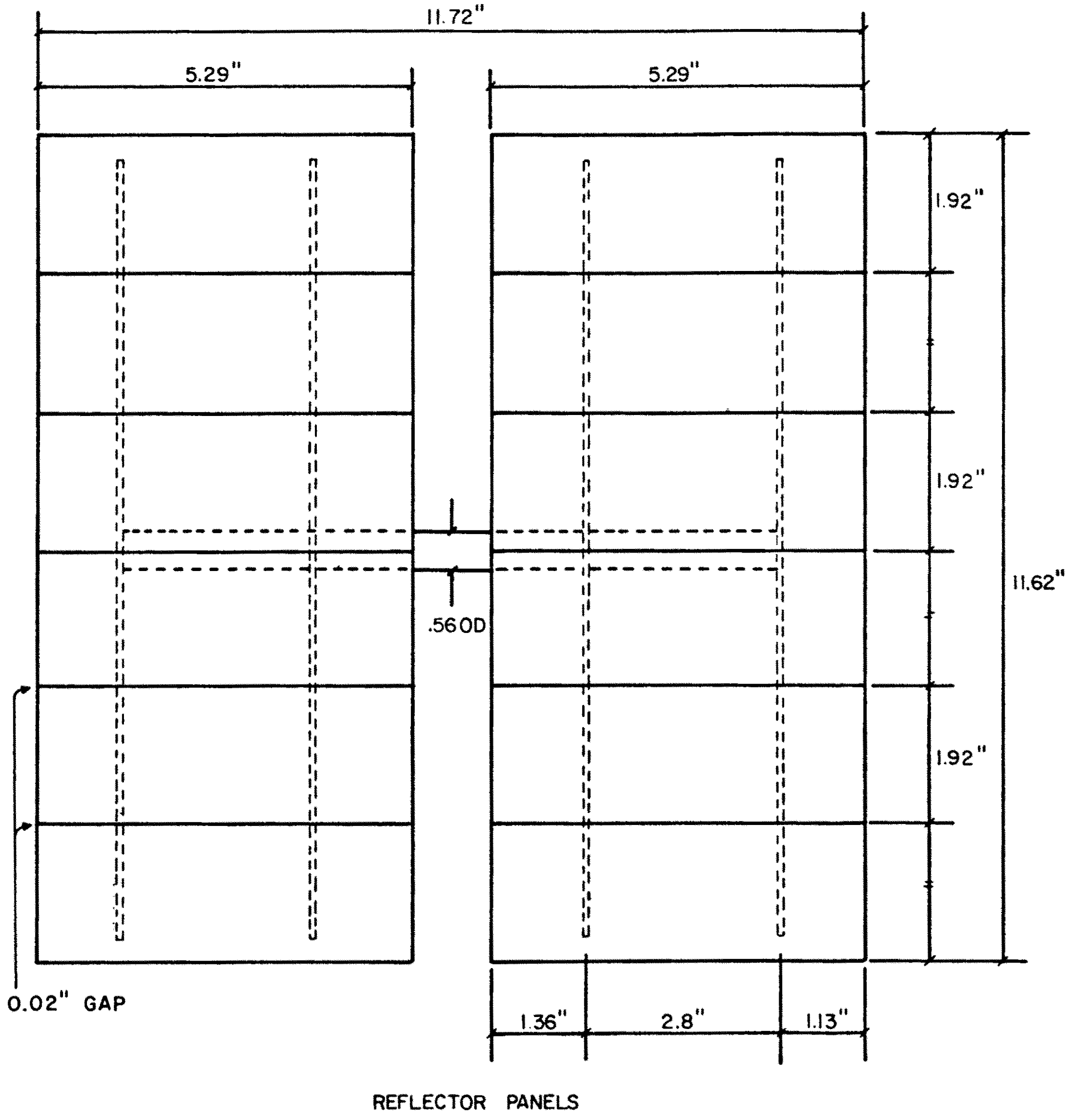

Figure 1b. Heliostat Test Model Dimensions

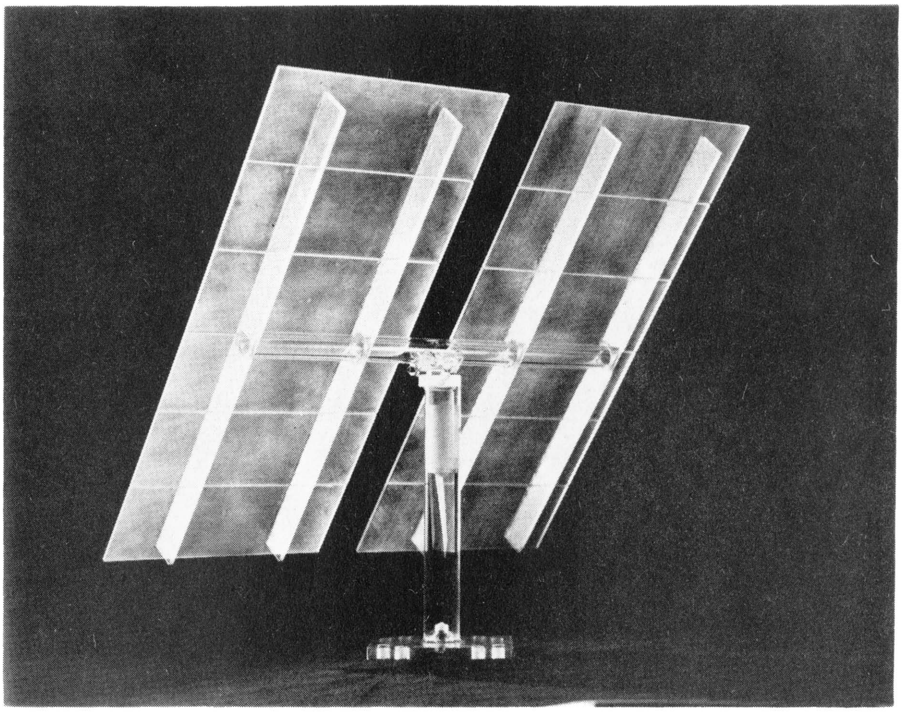

Figure 2. Photograph of the Wind-Tunnel Model

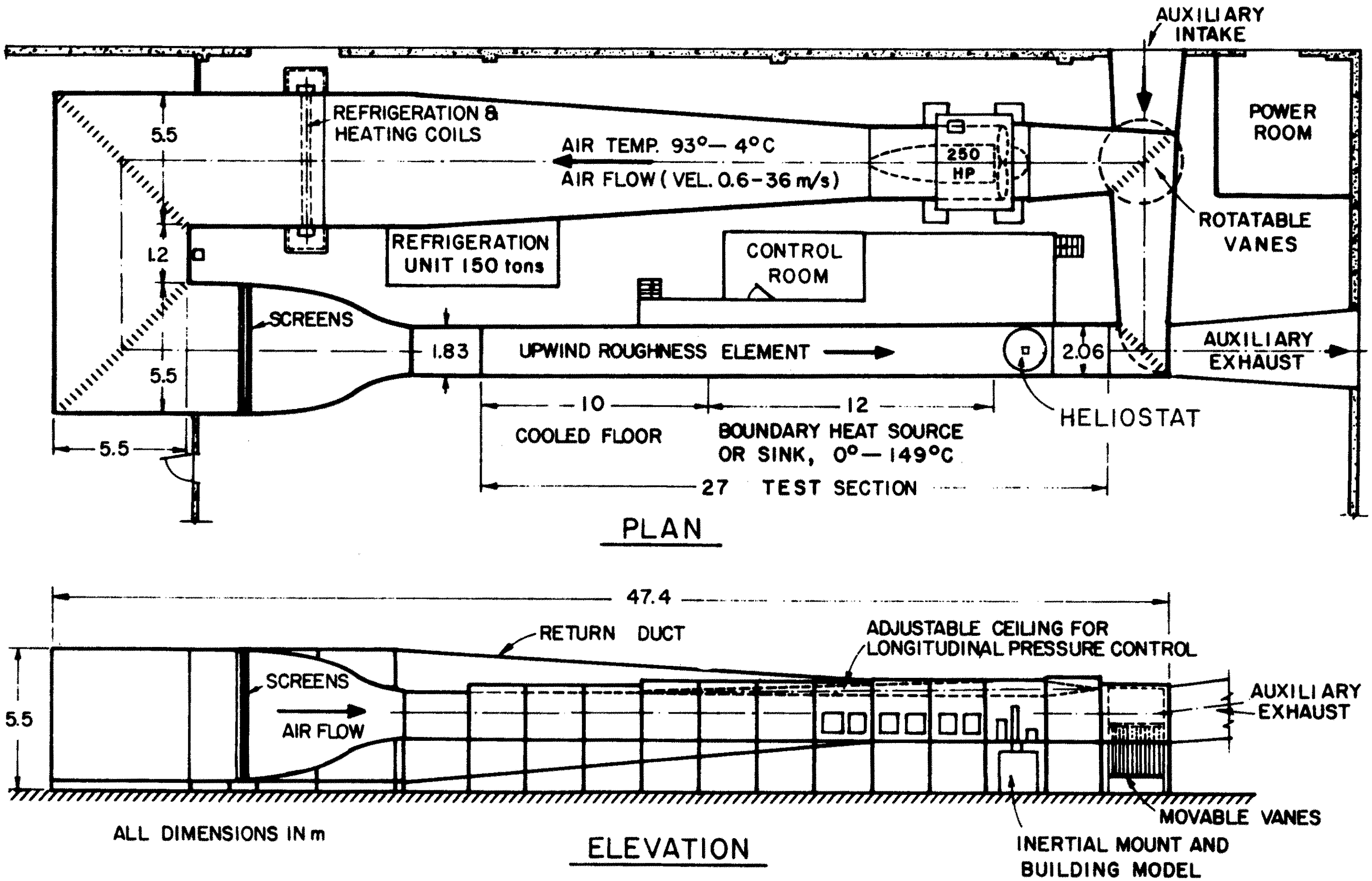

Figure 3. Meteorological Wind Tunnel

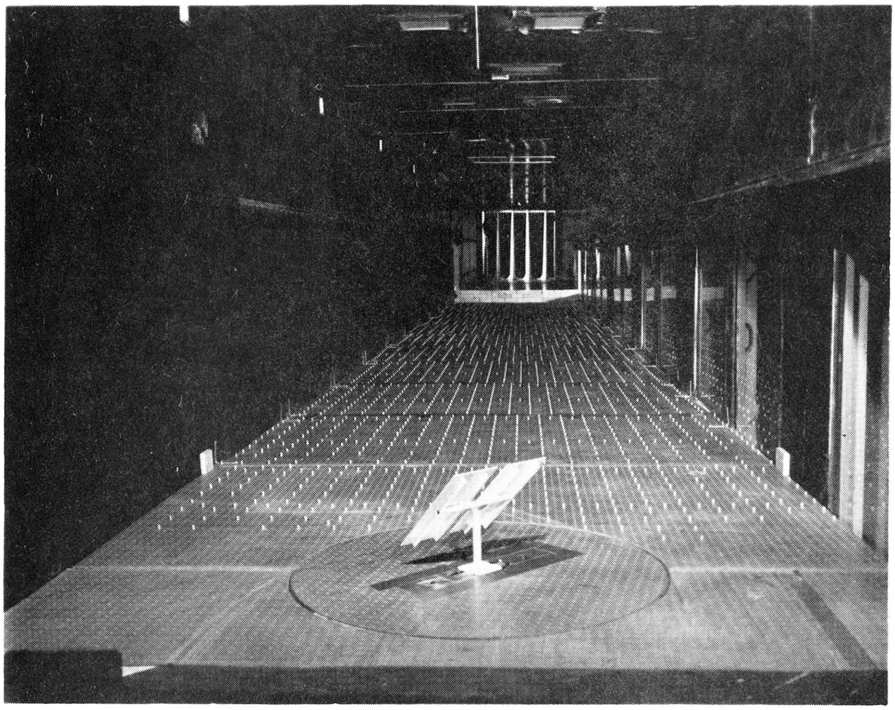

Figure 4. Model Installed in the Meteorological Wind Tunnel

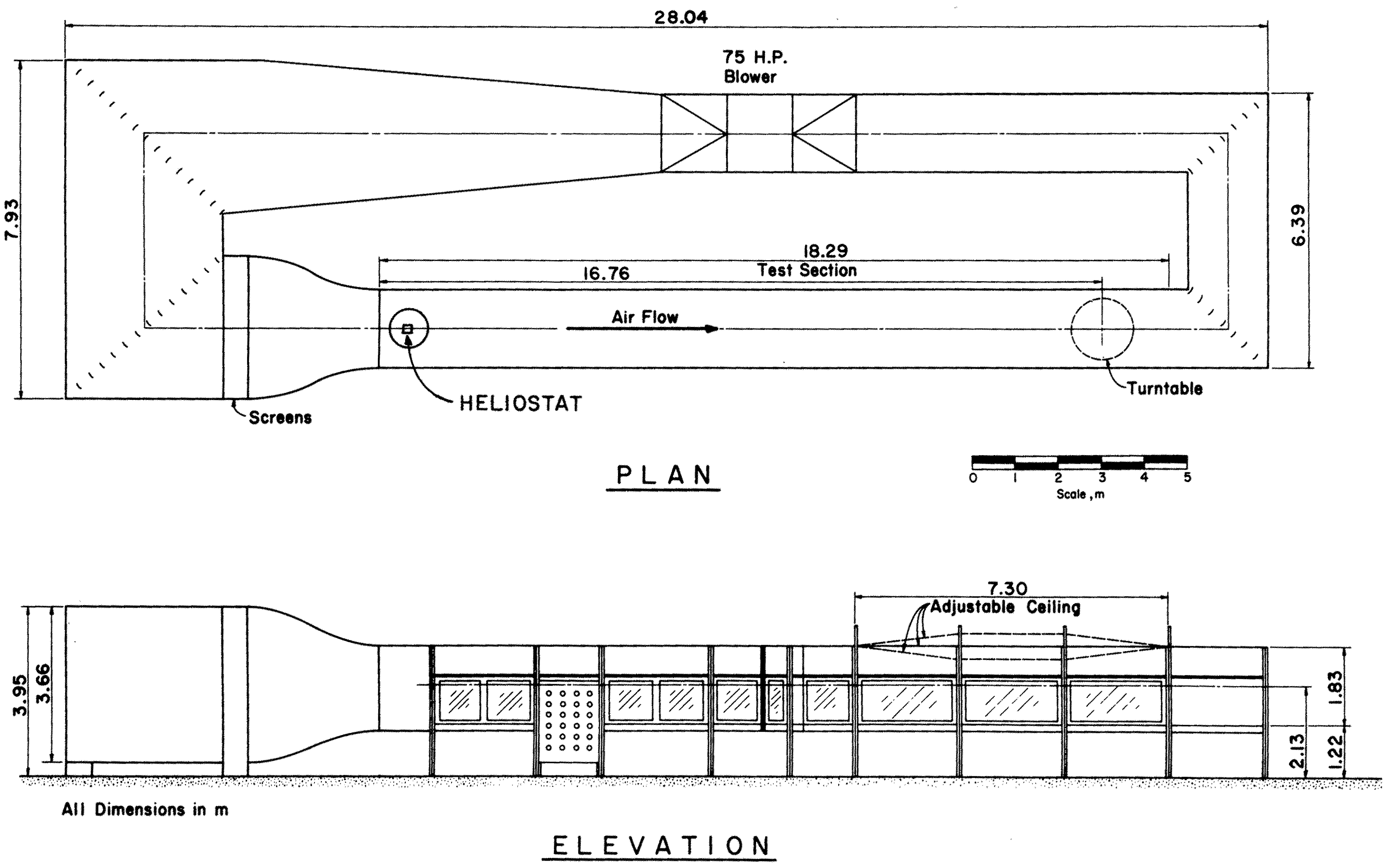

Figure 5. Industrial Aerodynamics Wind Tunnel

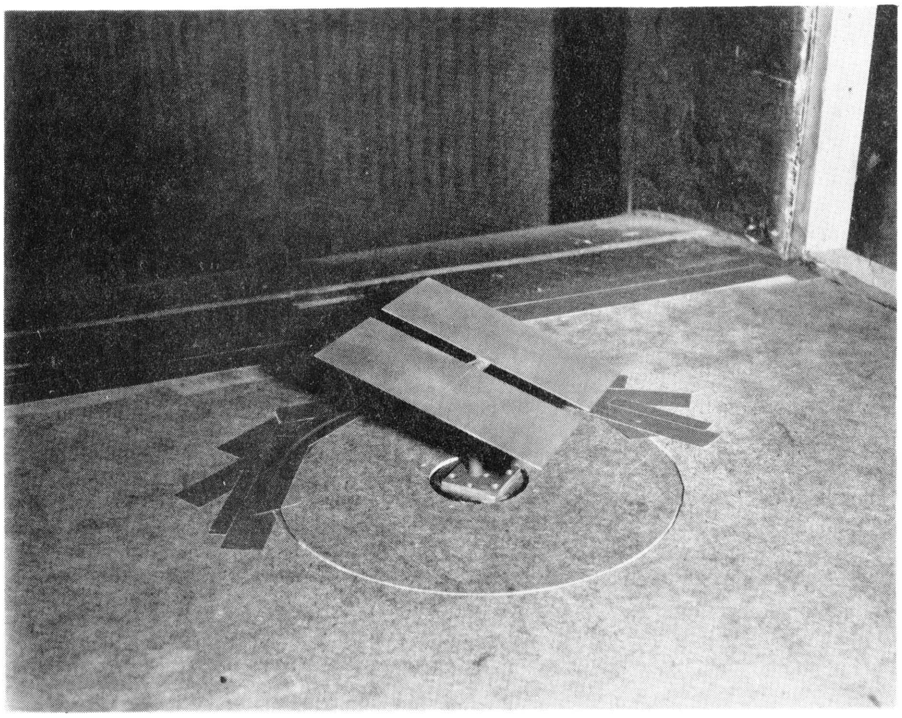

Figure 6. Model Installed in the Industrial Aerodynamics Wind Tunnel

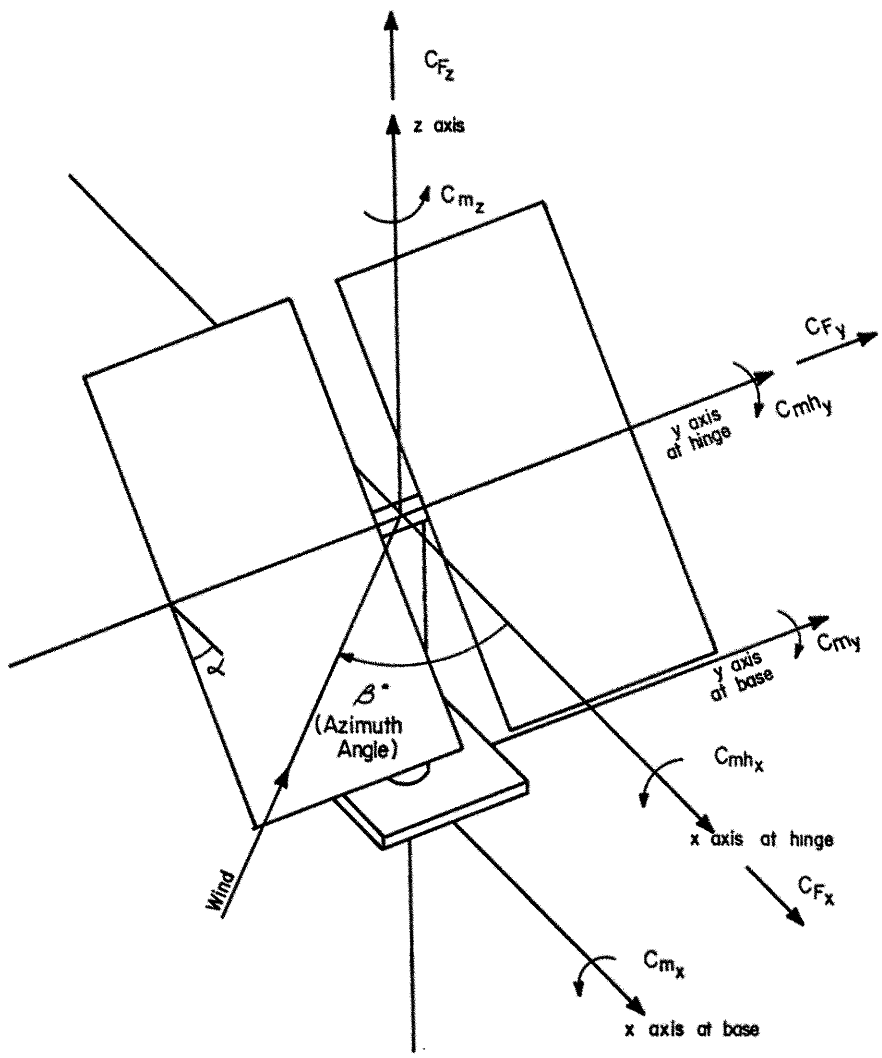

Figure 7a. Coordinate System on the Model

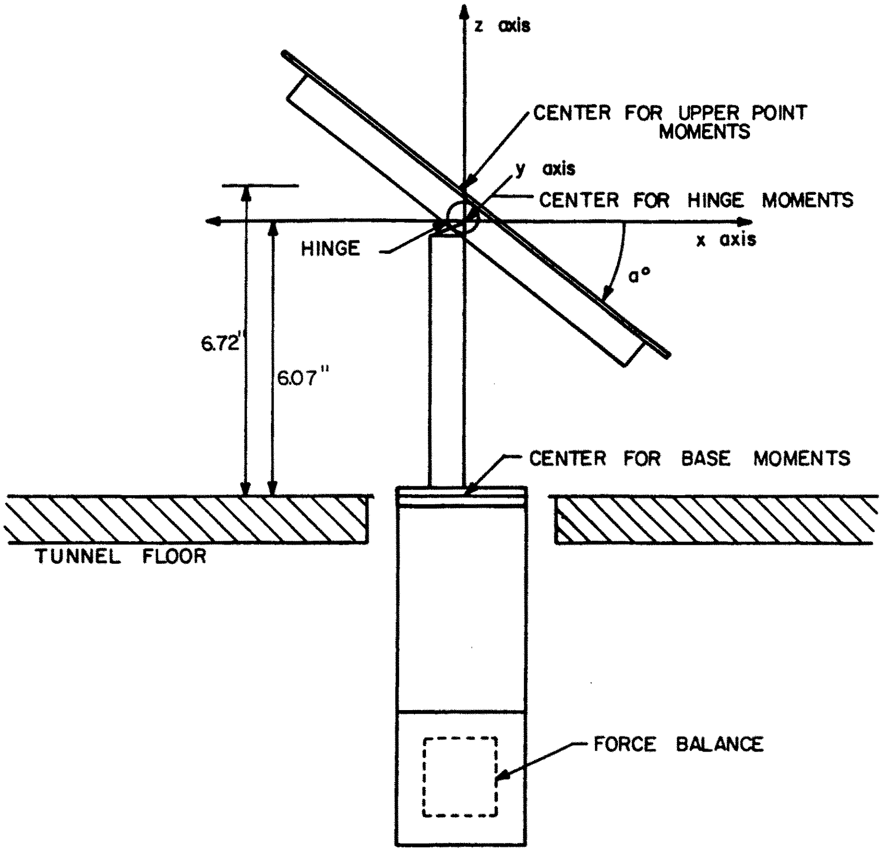

Figure 7b. Coordinate System on the Model

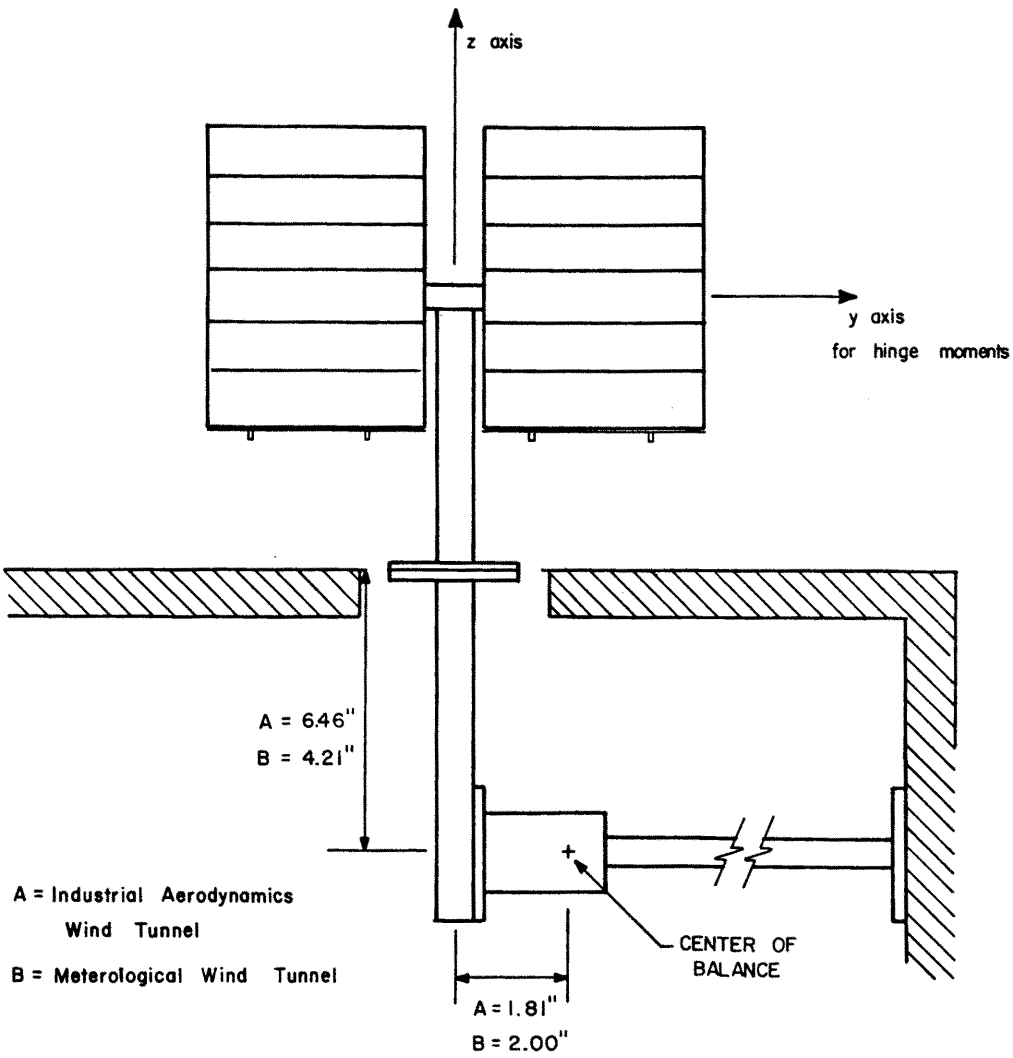

Figure 7c. Coordinate System on the Model

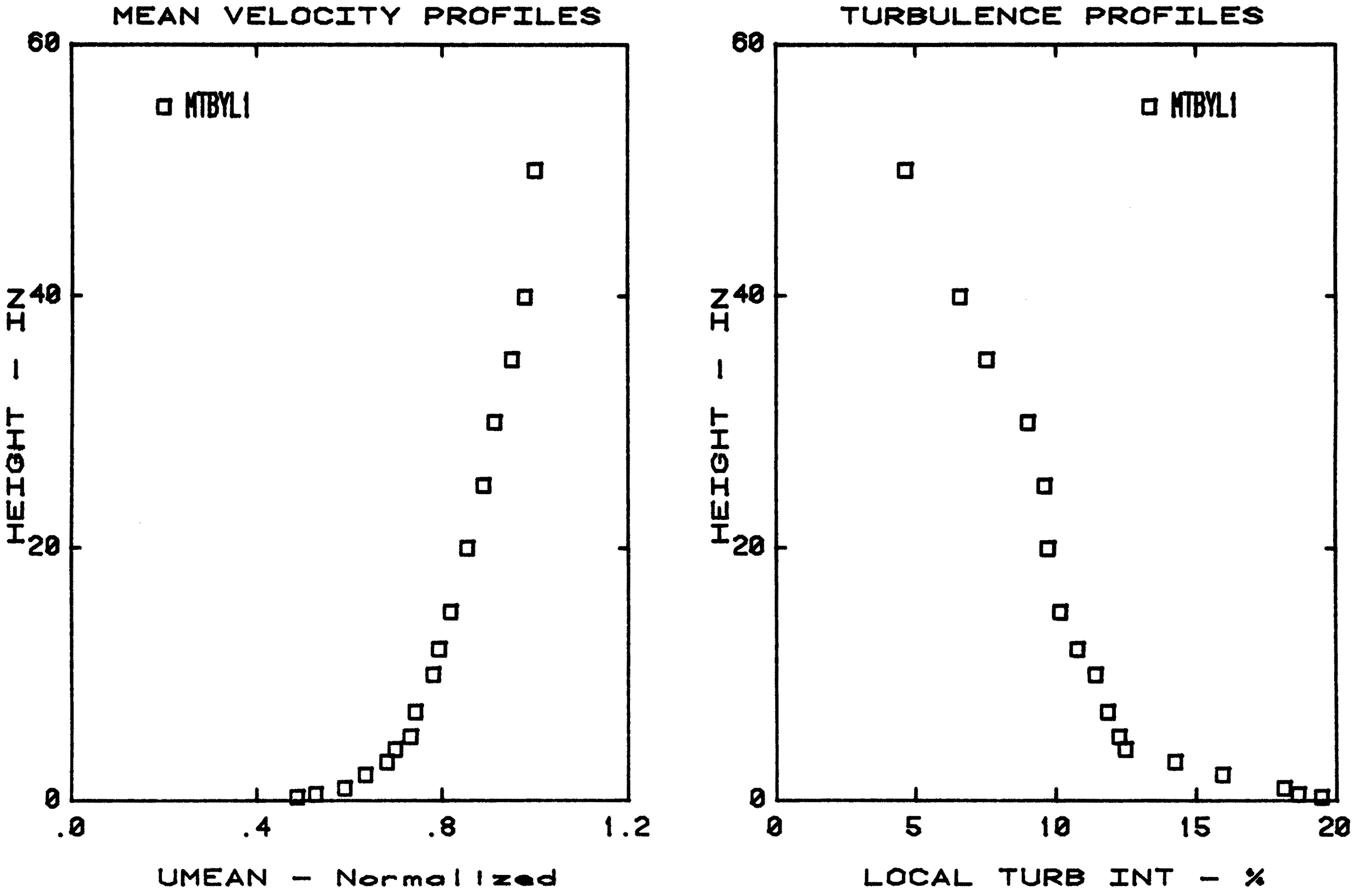

Figure 8. Velocity Profile in the Meteorological Wind Tunnel at Model Location

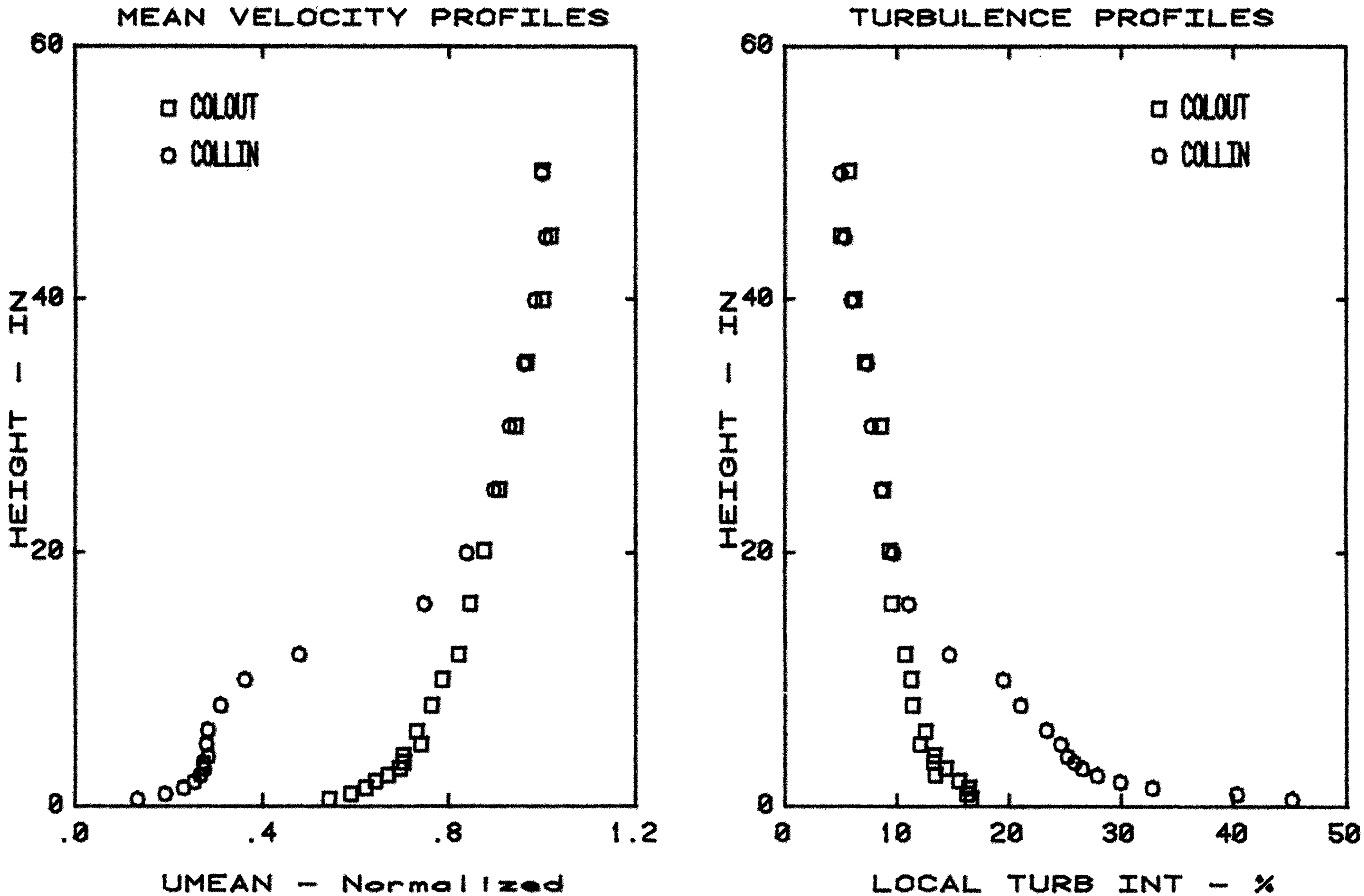

Figure 9. Velocity Profiles in Front of Heliostat in the Meteorological Wind Tunnel with Heliostat in Place and Removed

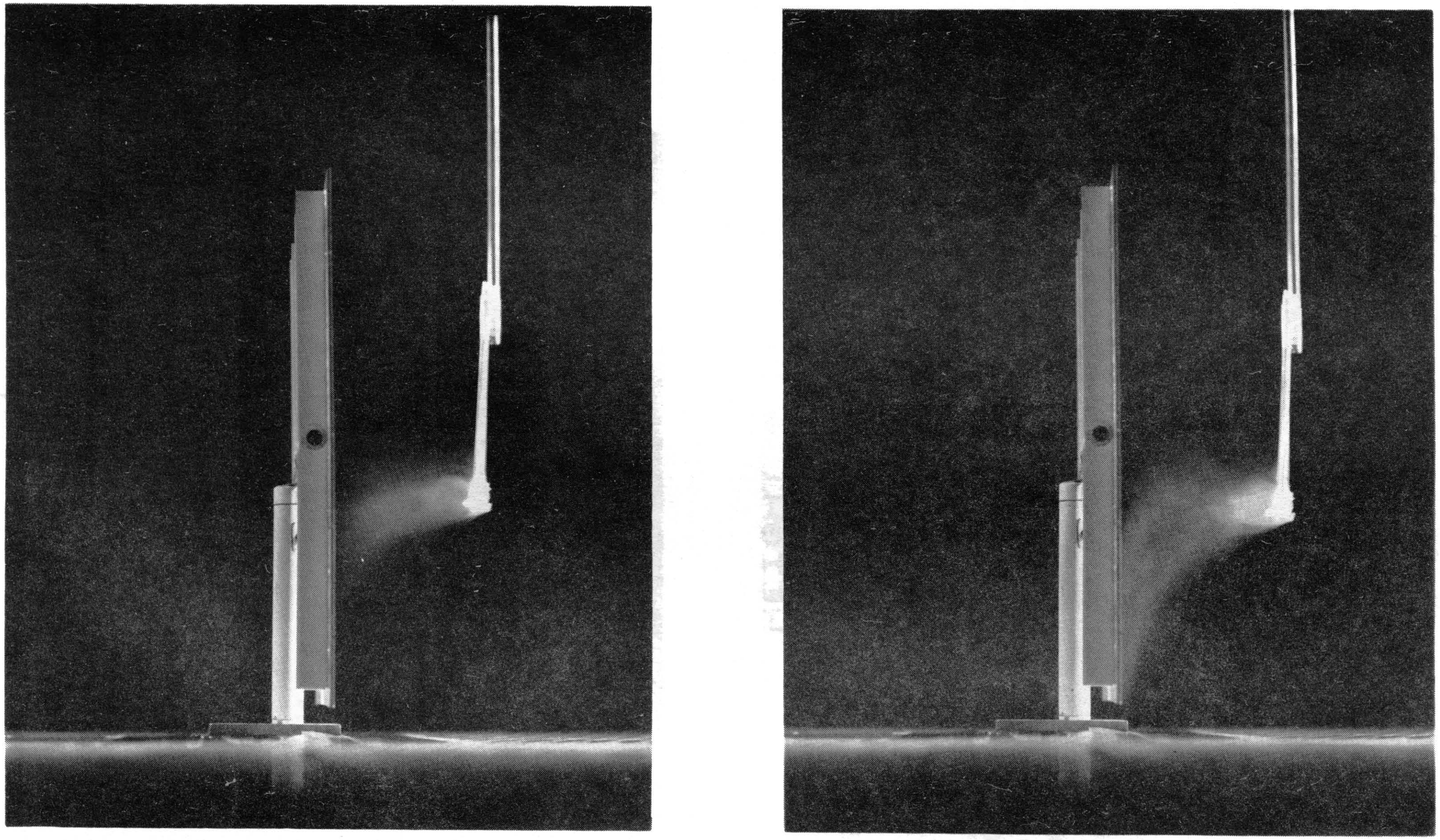

Figure 10a. Flow Visulaization Photographs in the Boundary Layer Flow

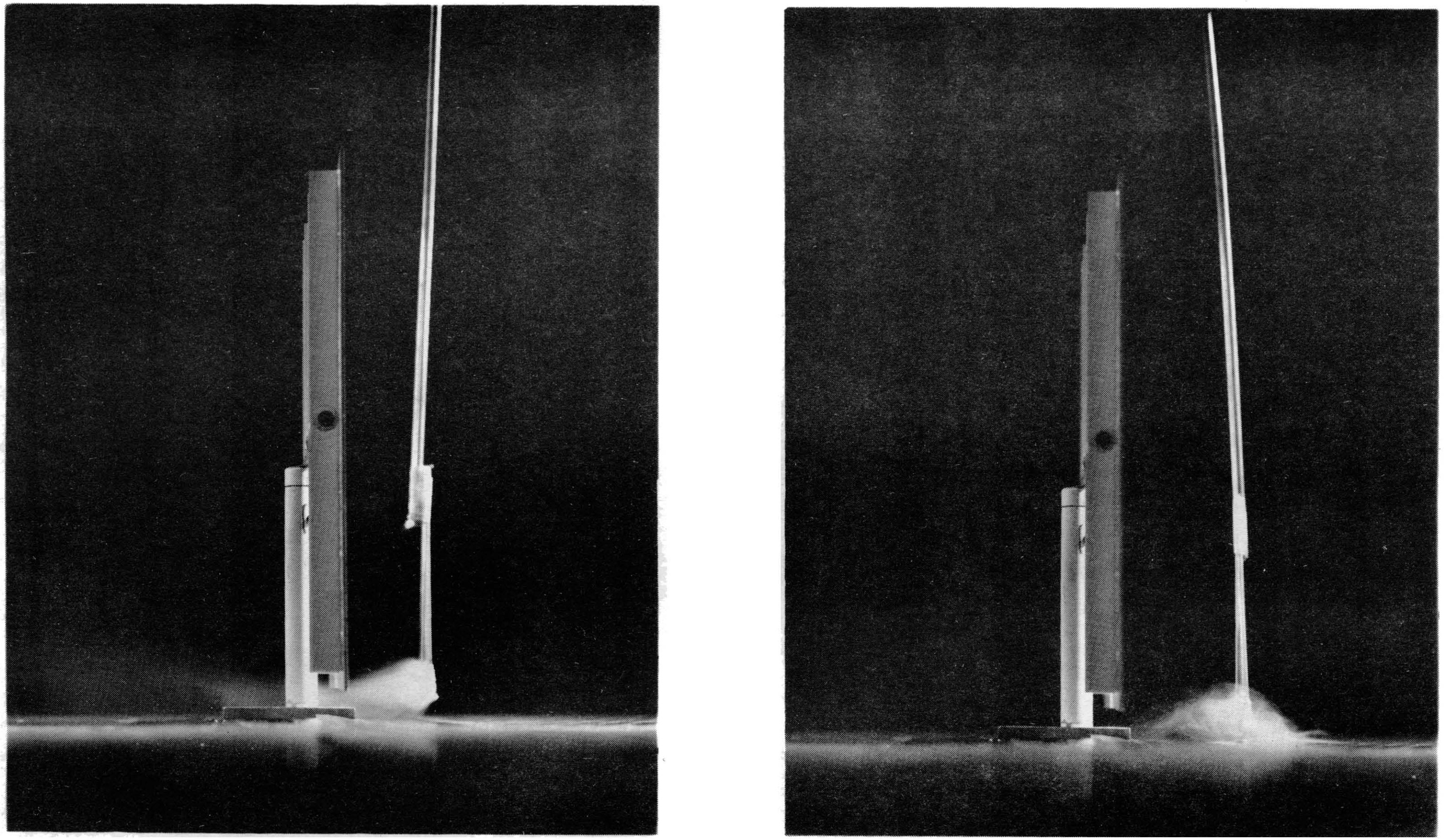

Figure 10b. Flow Visualization Photographs in the Boundary Layer Flow

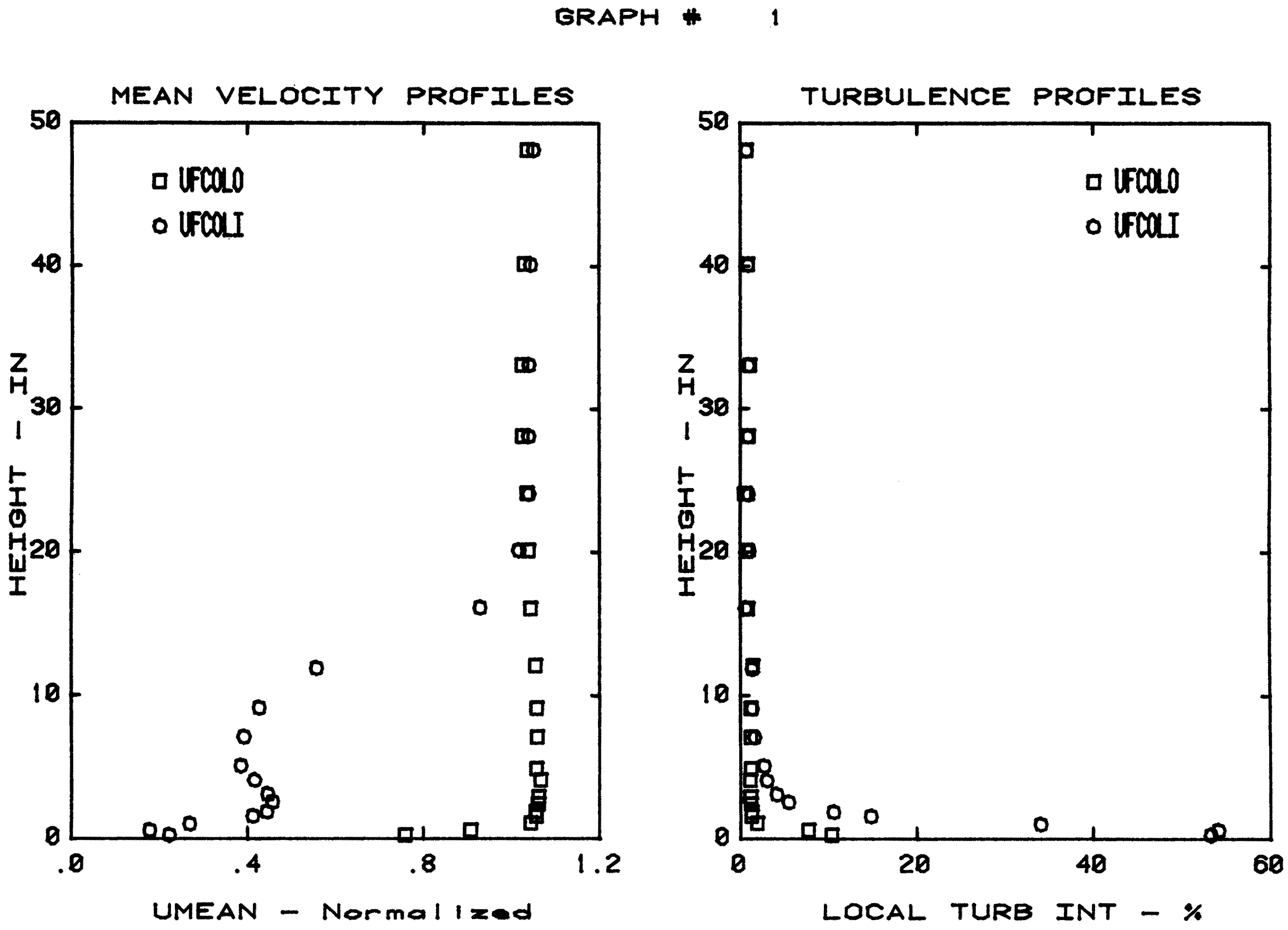

Figure 11. Velocity Profiles in Front of Heliostat in the Meteorological Wind Tunnel with Heliostat in Place and Removed.

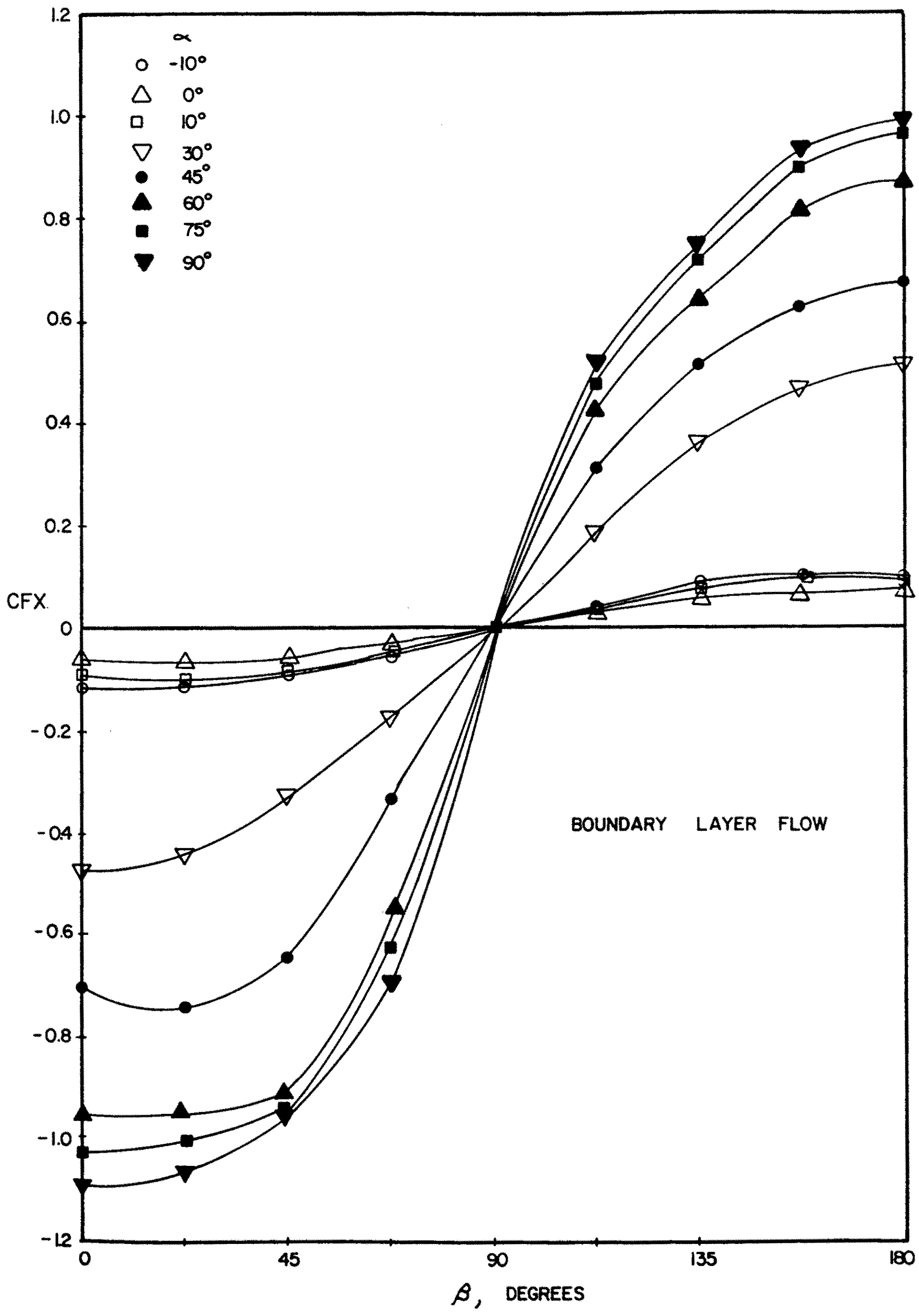

Figure 12a. Force Coefficient CFX as a Function of Wind Angle β and Tilt Angle α for the Boundary Layer Flow

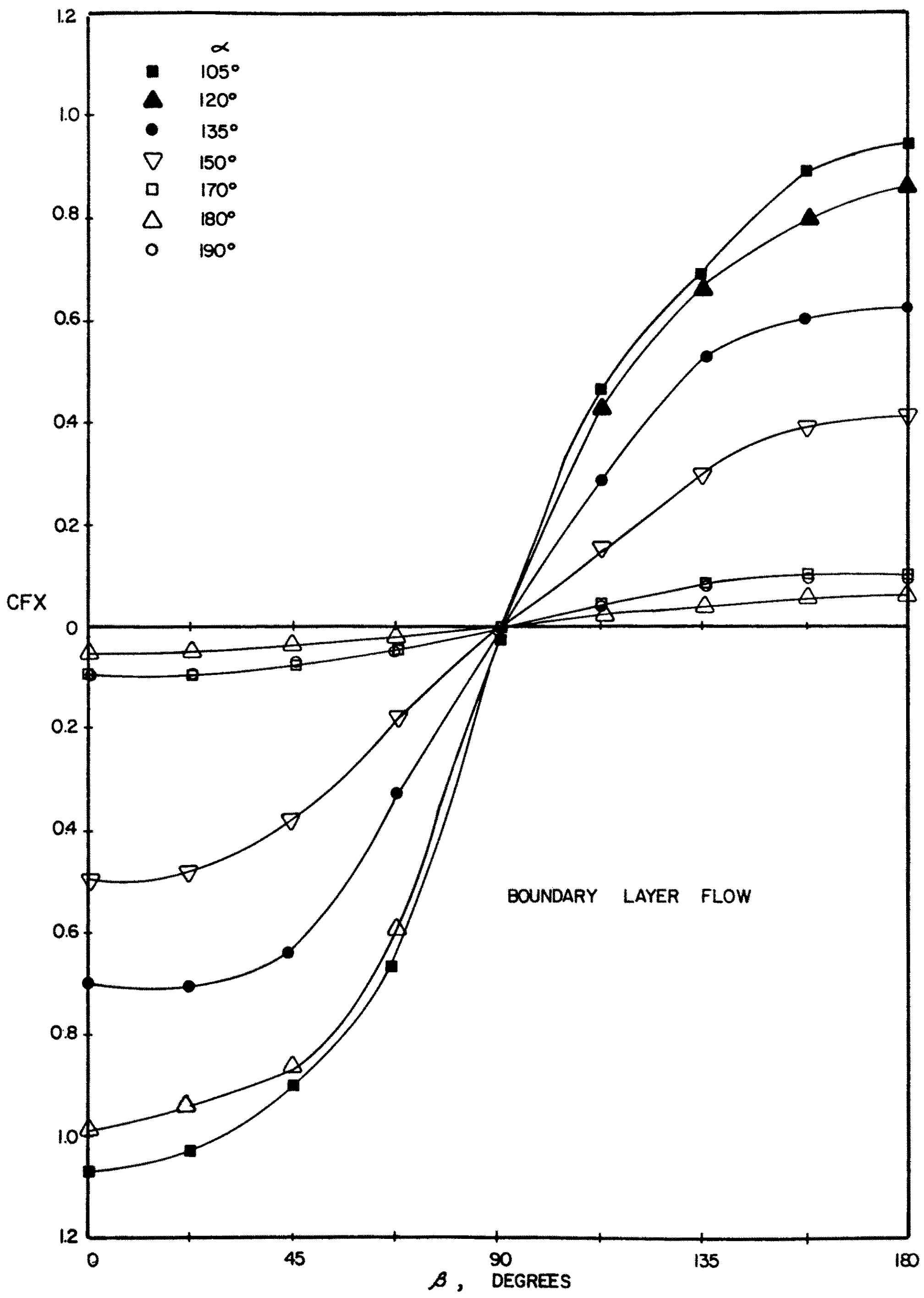

Figure 12b. Force Coefficient CFX as a Function of Wind Angle β and Tilt Angle α for the Boundary Layer Flow